THE UNIVERSITY OF MICHIGAN

INDUSTRY PROGRAM OF THE COLLEGE OF ENGINEERING

PROPERTIES OF NEUTRAL STRANGE PARTICLES PRODUCED BY 1.1 BEV NEGATIVE PI MESONS

Carl D. Graves

A dissertation submitted in partial fulfillment
of the requirements for the degree of
Doctor of Philosophy in the
University of Michigan
1958

February, 1958

IP-268

Doctoral Committee

Professor Donald A. Glaser, Chairman
Associate Professor John W. Carr, III
Professor Wayne E. Hazen
Associate Professor Paul V. C. Hough
Professor George E. Uhlenbeck

ACKNOWLEDGMENTS

Many people contributed to the success of this experiment and I would like to express my sincerest thanks to them. In particular:

To Professor Donald Glaser who first and foremost made this experiment possible.

To Professor Martin Perl for his open office door and many hours of physics talk.

To John Brown and Richard Hartung for their help in carrying out the experiment.

To Elsie Brown, my most dependable assistant, for her untiring efforts in my behalf.

To our scanners Sharlene Nelson and Harriet Rose who managed to smile while staring 30,000 pictures in the face.

And to my wife Eleanore, for her confidence and understanding throughout this work.

Finally I wish to thank the Engineering College-Industry Program for their help in the preparation of this manuscript.

TABLE OF CONTENTS

LIST OF FIGURES

LIST OF FIGURES CONT'D

LIST OF SYMBOLS

α_Λ = The probability that the Λ° decay by its normal charged mode.

γ = Gamma ray, i.e., electromagnetic radiation.

θ = Production or decay angle of V° particles.

θ° = Neutral strange particle with mass of about 965 electron masses, i.e., a K meson.

K = Any one of the strange particle mesons with mass of about 965 electron masses.

Λ° = Neutral strange particle with mass of about 2181 electron masses, i.e., a hyperon.

μ = Elementary particle (meson) with mass of about 207 electron masses.

Ξ = Strange particle with mass of about 2586 electron masses, i.e., a hyperon.

π = Elementary particle (meson) with mass of about 273 electron masses.

σ = Total cross section for a particle reaction.

Σ = Strange particle with mass of about 2323 electron masses, i.e., a hyperon.

φ = Decay angle of a V° particle.

N = Total number of pions entering the chamber

n = Total number of V° events

$N_{\Lambda\theta}$ = The number of hydrogen events found where both the Λ° and θ° decayed in the chamber.

N_Λ = The number of hydrogen events found where only the Λ° decayed in the chamber.

n_A = The number of events in the fraction of pictures scanned by A.

n_A' = The number of events found by scanner A.

P_Λ = Probability the a Λ°, decaying by its normal charged mode, decays before leaving the chamber.

p = Elementary particle with mass of about 1836 electron masses, i.e., a proton.

T_A = Scanning efficiency of scanner A.

V° = Any one of three neutral strange particles θ°, Λ°, or $\Sigma^\bullet$.

I. INTRODUCTION

In 1947 a new class of elementary particles was discovered, the so called strange particles. These particles are elementary in the sense that they are not composites of other particles in any known way, and they are particles in the sense of having the properties of unique mass and charge. Previously all elementary particles (with the exception of the massless photon and neutrino) were uniquely characterized by their rest mass and their charge. This is probably true of strange particles also. There are two categories of strange particles, the K-mesons with rest masses of about 965 electron masses, and the hyperons with rest masses between 2200 and 2600 electron masses. These new particles possess all three charge states, plus, minus and neutral. They are all unstable with lifetimes in the range of 10^{-8} to 10^{-10} seconds. The name "strange particles" has been applied to them primarily because of their anomalously long lifetimes. To understand why their lifetimes are considered anomalous, we must first examine the characteristics of particle interactions.

Particle interactions can be divided into three classes based upon their "strength". The Yukawa or nuclear interaction is the strong interaction which holds the nucleus together and is responsible for pion production. It is also called a "fast" reaction since the processes associated with it take place on a time scale of about 10^{-23} seconds. Next is the electromagnetic interaction which is something like 10^{-2} times weaker. It is characterized by a time scale of about 10^{-21} seconds and is responsible for photon emission and forces involving electric charges.

Finally there is the Fermi type interaction which is some 10^{-14} times weaker than the strong interaction and characterized by a time scale of about 10^{-9} seconds. It is responsible for beta-decay and the decay of pions and muons. The production of strange particles belongs to the class of strong interactions while their decay belongs to the class of weak interaction. But according to one of our most fundamental ideas, a particle made in a strong interaction should decay that way. From this paradox the name "strange" particles originated.

An "explanation" of this paradox was proposed by Pais[2]. The idea, known as associated production, was that the strong interactions which produce strange particles work only on more than one strange particle at a time and thus strange particles are made in groups of two or more. Once separated after production the strange particles live a long time before decaying into conventional particles via the weak interaction. The next step was the introduction of a conservation law by Gell-Mann[3] and Nishijima[4] to account for associated production. They extended the concept of isotopic spin, so successfully used in formulating the charge independent nature of nuclear interactions, to strange particles. The strange particles were arranged in charge multiplets and assigned values of total isotopic spin (T) and Z - component of isotopic spin (T_z). These quantities are supposed to be conserved in strong interactions. Then a new intrinsic property, called strangeness, was assinged to every elementary particle. The ordinary particles were assigned a strangeness quantum number, S, of zero. The strange particles were assigned various values of $S = \pm 1$ and $S = -2$ and it was proposed that the total strangeness be conserved in strong and electromagnetic interactions. According to their scheme all

the hyperons (Λ and Σ) except the cascade particles (Ξ) have S = -1. The cascade particles have S = -2. The K^+ and K° (θ° and τ°) mesons have S = +1 while the K^- and $\bar{K}^\circ$ (anti K° particle) have S = -1. The Λ° forms a charge singlet, the Σ^+, Σ° and Σ^- form a charge triplet and the Ξ^- and Ξ° form a charge doublet. The K meson pairs (K^+, K°) and (K^-, $\bar{K}^\circ$) each form charge doublets. It was further proposed that the strangeness quantum number was related to the charge (Q), baryon number (M) and Z-component of isotopic spin (T_z), by

$$Q = T_z + M/2 + S/2$$

The conservation of Q, T_z and M then implies the conservation of S in any reaction. These ideas have proved remarkably successful and there are no known cases of strong or electromagnetic interactions where strangeness conservation has been violated. The long lifetime of strange particles is then accounted for by the fact that strangeness is not conserved in their decay, i.e., in weak interactions.

The associated prodiction hypothesis was first experimentally supported by Shutt, et al.[5] and by Walker and Shephard[6] using a hydrogen diffusion cloud chamber and pion beams of 1 Bev and 1.4 Bev kinetic energy. The strange particle reactions which conserve strangeness at these pion energies are

1. $\pi^- + p \rightarrow \Lambda^\circ + \theta^\circ$
2. $\pi^- + p \rightarrow \Sigma^\circ + \theta^\circ$
3. $\pi^- + p \rightarrow \Sigma^- + K^+$

Twelve cases consistent with these reactions were found. A similar experiment by Budde, et al.[7] using a 6 inch propane bubble chamber and a 1.3 Bev

pion beam supported the above results and gave some additional information on the production and decay process. However, much more detailed information on these reactions and the intrinsic properties of these particles was needed. In an effort to obtain more information we have exposed a 12 inch propane bubble chamber to a 1.1 Bev π^- meson beam at the Brookhaven Cosmotron. Over 30,000 pictures were taken and a total of 150 events consistent with the above reactions were found.

The results of our experiment concerning the third reaction have been reported elsewhere as have the results on the first two reactions for those cases in which both the Λ° and θ° decay in the chamber[8]. Hence only the first two reactions will be considered here, and our results consist of only those cases where either the Λ° or θ° are seen to decay in the chamber, but not both. However, for completeness, the previously reported cases where both the Λ° and θ° decay in the chamber will be included in this thesis. We give the angular distributions and cross sections for the production of Λ°, θ°, and Σ° particles on free protons (i.e., hydrogen events), and the lifetimes and decay angular distributions of these particles. The probability of neutral decay and results concerning conservation of parity (in Λ° decay) and the intrinsic spins of these particles are also presented. In addition the conservation of isotopic spin in Σ hyperon production and isotopic spin selection rules in Λ° and θ° decay is discussed.

II. EXPERIMENTAL ARRANGEMENT

2.1 The Pion Beam

To study the strange particle reactions previously described it was necessary to take our large propane bubble chamber to the Brookhaven National Laboratory where a high energy π meson beam is available. A floor plan of the experimental arrangement is shown in Figure 1. The Brookhaven Cosmotron produces a circulating beam of 3 Bev protons. This proton beam was allowed to strike a graphite target placed in the field-free south straight section of the Cosmotron. The high energy protons interacting with the grpahite produced an energy spectrum of π mesons in all directions. The negatively charged π mesons were bent out of the machine by the Cosmotron magnetic field and a slit was made in the shielding wall at the appropriate place to pass pions whose momentum was 1.231 Bev/C (1.1 Bev kinetic energy).* To provide a precise momentum analysis the pion beam was then deflected by a steering magnet through a collimating slit in a shielding blockhouse wall and into our propane bubble chamber. The deflection by the steering magnet of 1.231 Bev/C pions was determined by the hot wire method and the momentum resolution of this pion beam was determined by a method described in reference 8. We found that half the beam fell in a momentum interval of $\pm$ 2% from the mean value. It was also estimated that about 8% of the beam particles entering the chamber were μ^- mesons (see Chapter V).

---

* We wish to thank R. M. Sternheimer of the Brookhaven National Laboratory for calculating the pion trajectory through the Cosmotron field.

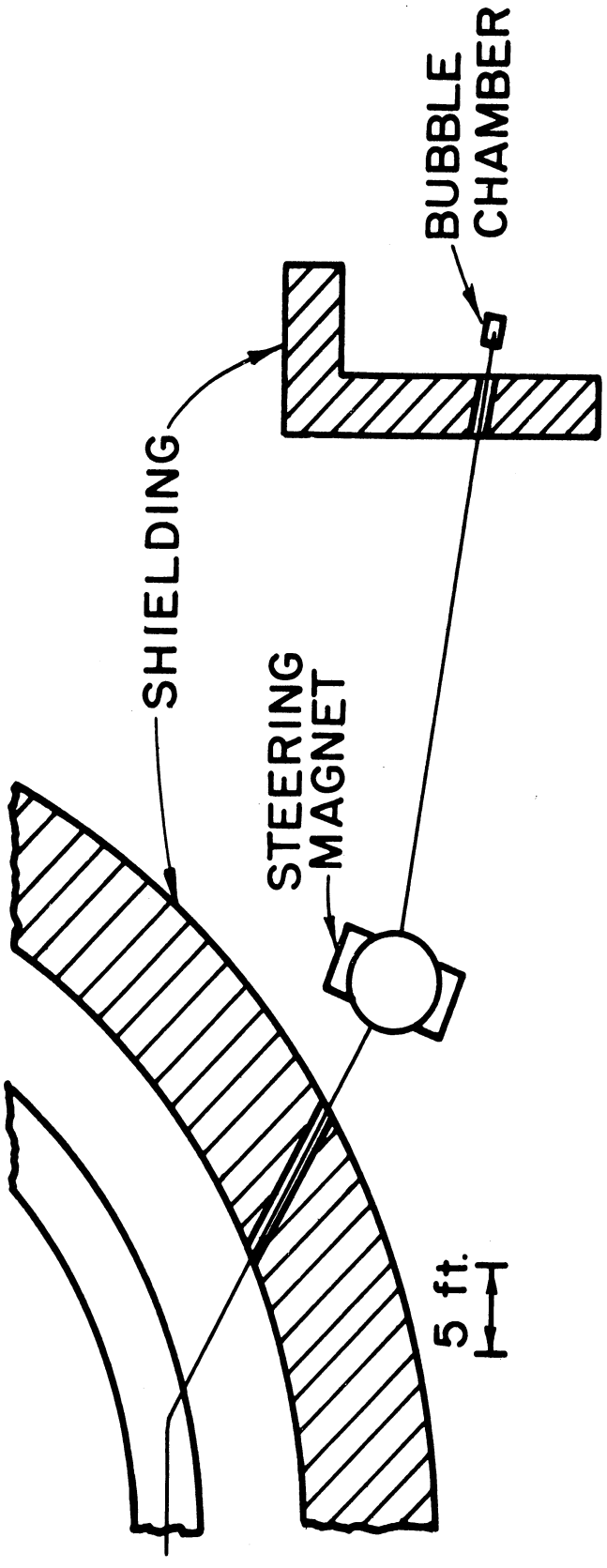

Figure 1. Plan View of Experimental Set-Up.

2.2 The Propane Bubble Chamber

A detailed description of the operation of a propane bubble chamber similar to ours has been given in reference 9. A description of the bubble chamber used in this experiment has also been presented elsewhere[8]. The sensitive volume of our chamber was a rectangular region 5 x 5 x 12 inches with the beam traversing the long dimension. A schematic drawing of the chamber is given in Figures 2 and 3. The chamber was operated at a temperature of 51.9°C and at a pressure of 375-400 psi. The oven surrounding the chamber contained heaters and fans to circulate the heated air. Temperature was controlled by means of a thermistor. Compressed air applied to a diaphragm in contact with the propane provided the needed pressure on the liquid and expansion was obtained by a 3/4 inch Barksdale valve actuating a large poppet valve. Two 70 mm cameras with matched lens were rigidly mounted on a steel I-beam frame and provided with pressure film holders and a vacuum film backing to insure uniform stereo photography of the chamber (Figure 4). The use of a Fresnel lens and a line source of light with a flash duration of about 40 microseconds gave excellent illumination throughout the whole chamber for bright field photography. Finally to provide an accurate method of converting measurements made on the stereographic negatives to real space coordinates, a rectangular array of fiducial marks was deposited on the inner surface of the front and back glass windows. The fiducial marks were spaced 1.000 $\pm$ 0.002 cm. from each other.

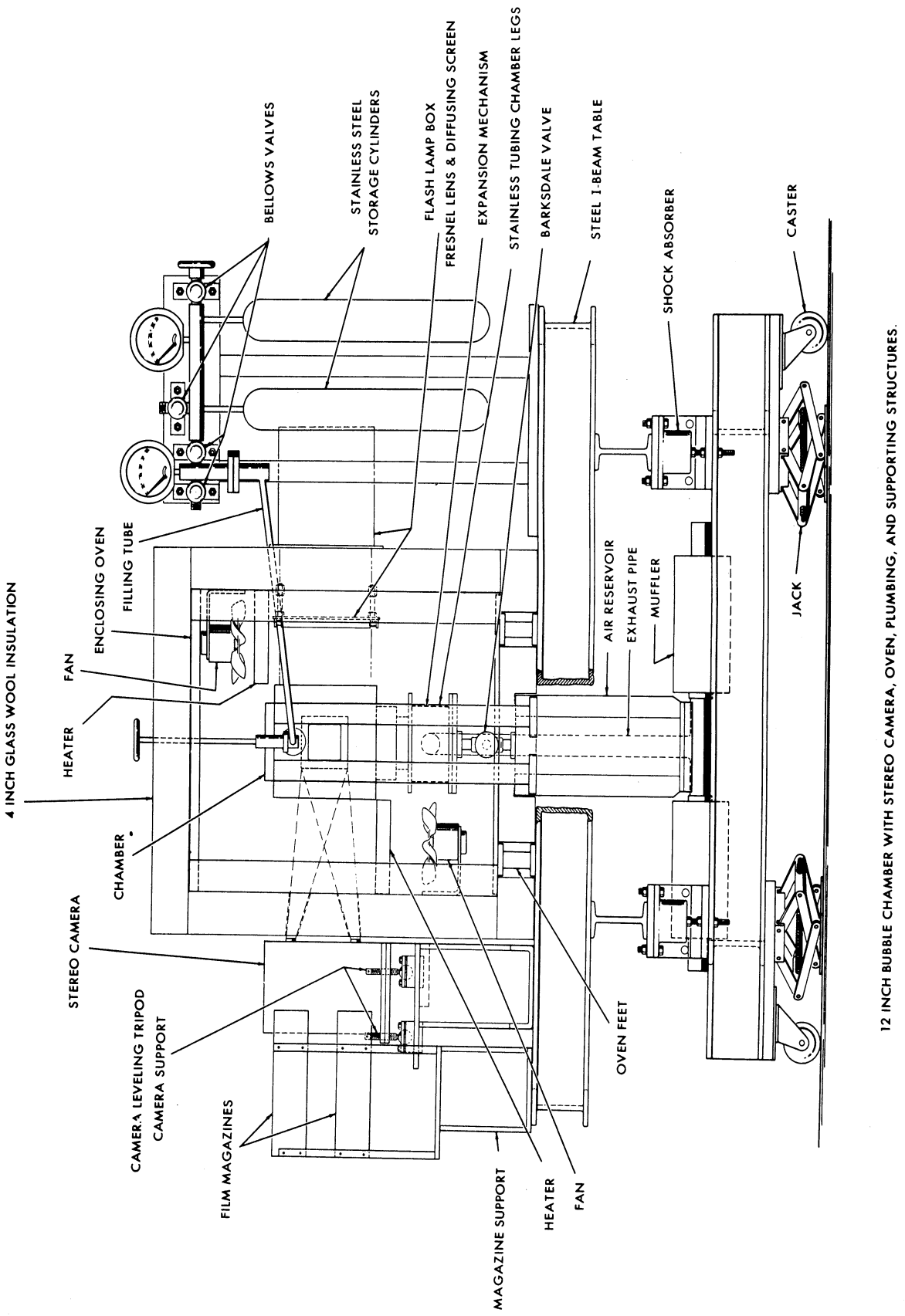

Figure 2. Overall Schematic Drawing of Bubble Chamber Assembly.

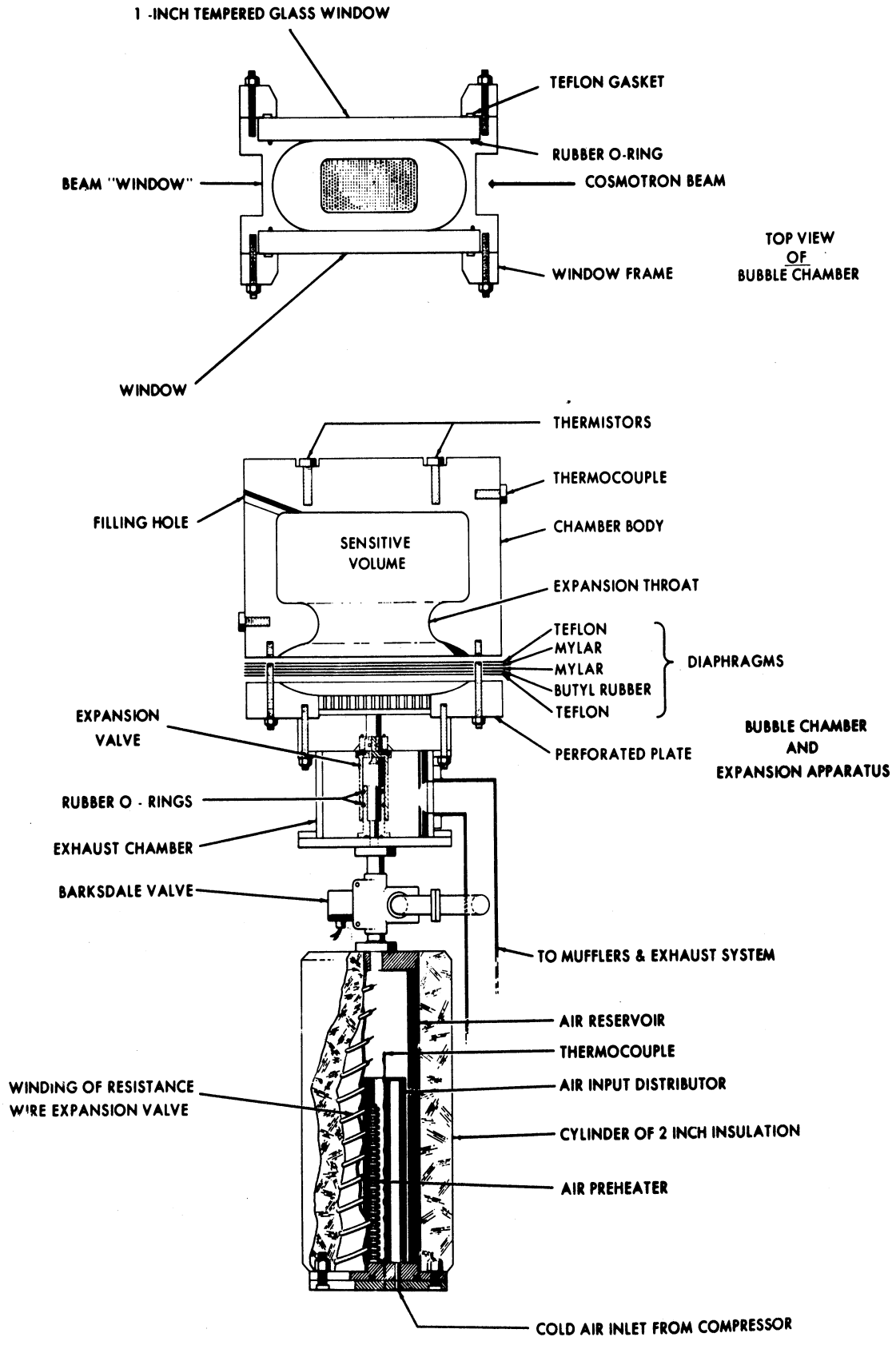

Figure 3. Detail Schematic Drawing of Chamber Proper.

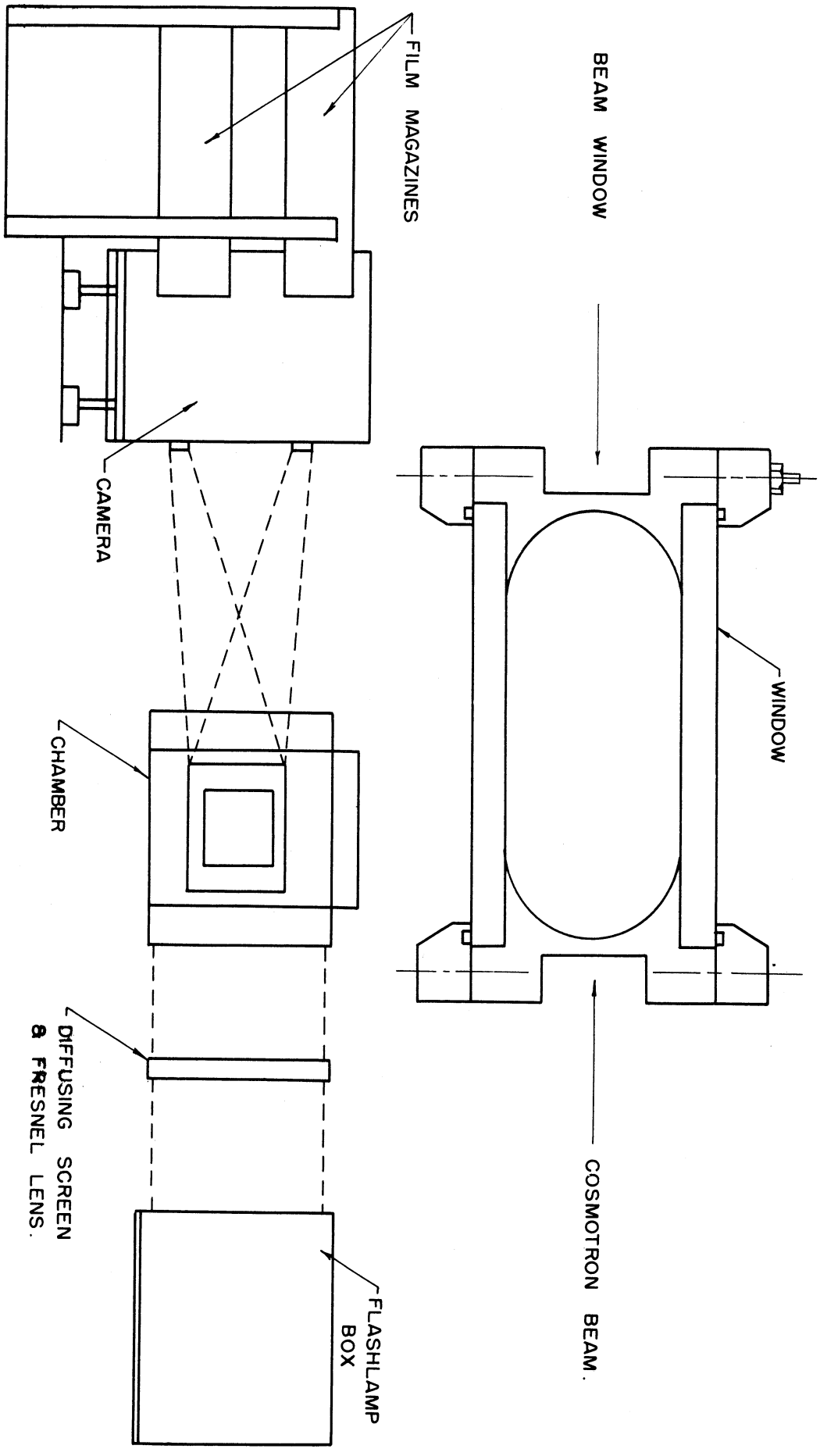

Figure 4. End and Top Views of Bubble Chamber.

III. REDUCTION OF FILM DATA

3.1 Scanning

As a result of previous experiments (Chapter I), the strange particle productions we could expect to find using the π^- meson beam described were:

1. $\pi^- + p \rightarrow \Lambda^\circ + \theta^\circ$
2. $\pi^- + p \rightarrow \Sigma^\circ + \theta^\circ$
3. $\pi^- + p \rightarrow \Sigma^- + K^+$

The third reaction has been discussed elsewhere[8] and will not be considered in this thesis. The normal charged decay modes of the neutral strange particles produced in reactions one and two are

$$\Lambda^\circ \rightarrow \pi^- + p,$$

$$\theta^\circ \rightarrow \pi^- + \pi^+,$$

$$\Sigma^\circ \rightarrow \Lambda^\circ + \gamma.$$

The normal lifetime of the Λ° and θ° is about 10^{-10} seconds, and the Σ° about 10^{-21} seconds. There was also a possibility that the Λ° and θ° particles could decay by a long lived or neutral mode which would not in general be visible in our chamber. (The alternate decay modes are discussed in Chapter V.) The decay of the Λ° and θ° particles would appear on our sterographic negatives as V shaped tracks, each leg of the V being a charged secondary resulting from the decay of the neutral strange particle primary. Since the Σ° decays with such a short lifetime, $\Sigma^\circ - \theta^\circ$ events would look the same as $\Lambda^\circ - \theta^\circ$ events to our scanners. Hence to find V° events our scanners were instructed to scan along each incoming pion beam track. If a pion track appeared to end inside the

chamber with no visible interaction, a search was made for associated V - shaped tracks which opened away from the ending pion and where a line joining the ending pion and the vertex of the V passed inside the V. This insured the possibility of conserving momentum in the decay process.

Approximately 30,000 pictures with an average of about 16 pion tracks per picture were scanned in this manner by the three scanners under our supervision. Each scanner averaged 200 pictures a day and possible events were found at a rate of about one in every fourth picture. Possible events were then examined by us and about a third of them rejected. Events were rejected for such things as a very short recoil track off the ending pion track, confusion of electron pairs with decaying V^{O}'s or on the basis of bubble density. The remaining possible V^{O} events were then subjected to a detailed analysis.

3.2 Measurement and Computation

Since the final determination of V° events was primarily based upon satisfying kinematical requirements, it was necessary to determine the real space production and decay angles of events found in the scanning. To accomplish this, measurements were made on the stereographic pair of film negatives of selected points on each event (Figure 6). The measurements were made using a traveling microscope arrangement which read to the nearest 0.001 inch. The results of the measurements were punched on IBM cards for processing by an IBM 650 computer. A typical event required two IBM cards of input data.

To obtain the relevant production and decay angles it was first necessary to compute the real space coordinates of the selected points on

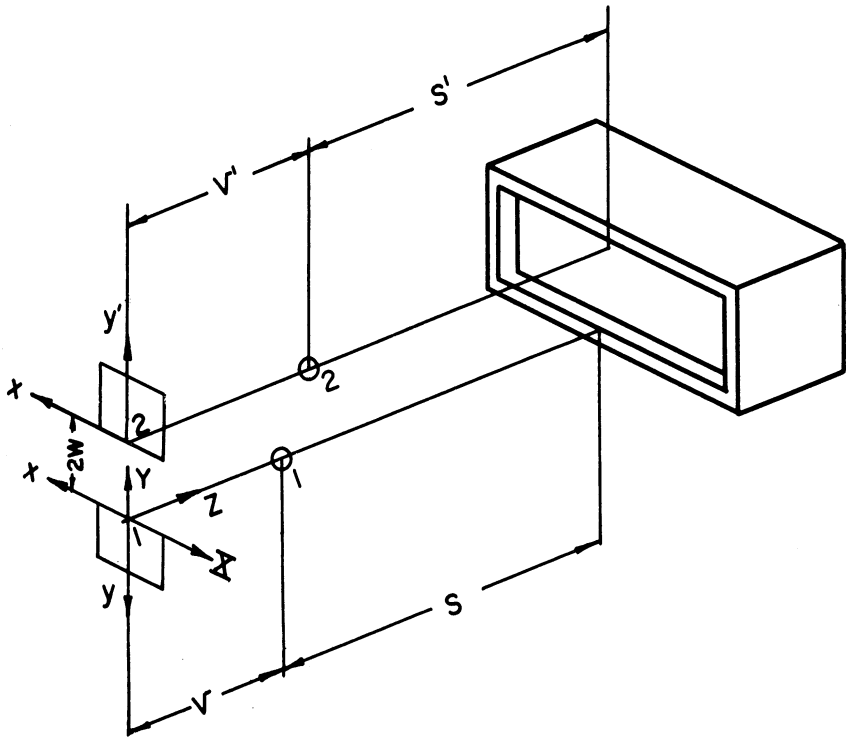

Figure 5. Stereo Camera-Bubble Chamber System.

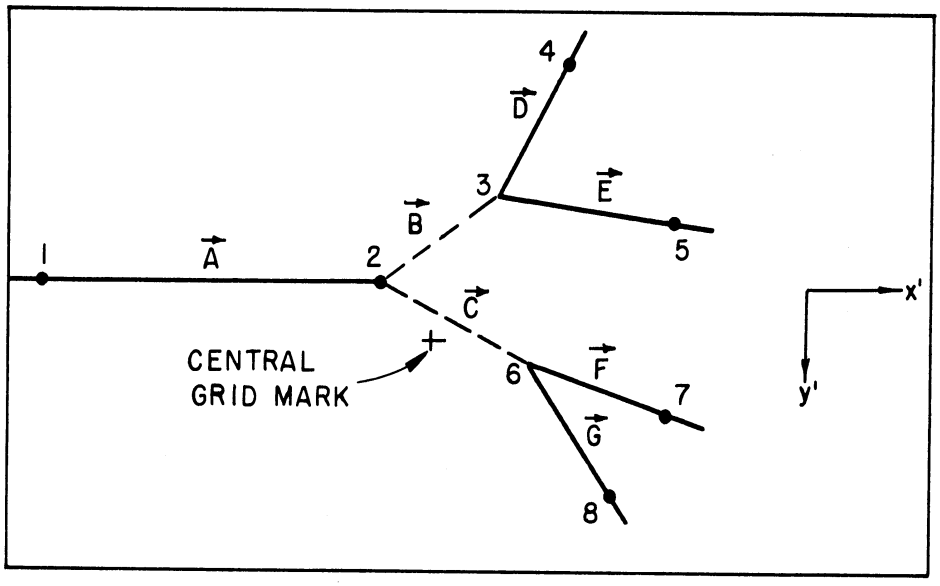

TOP CAMERA VIEW

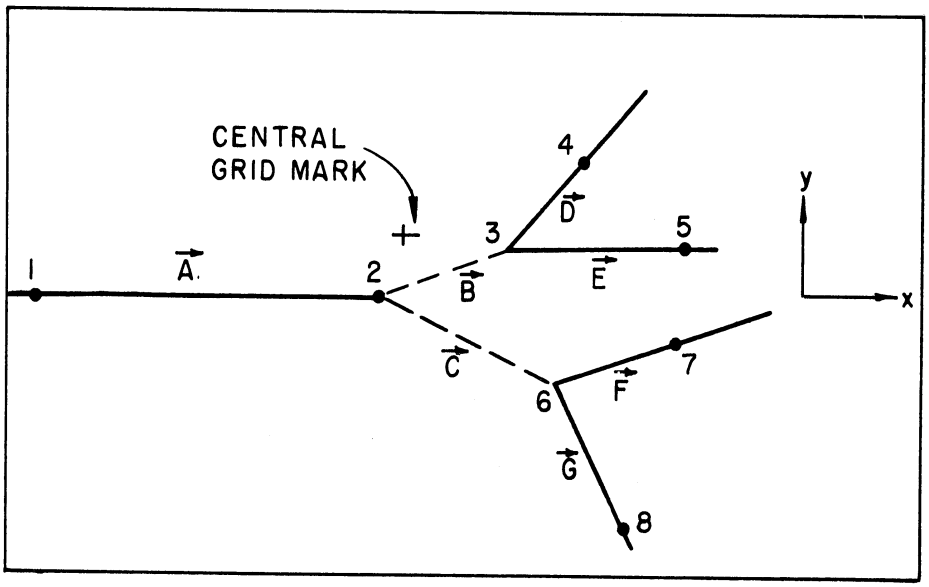

BOTTOM CAMERA VIEW

Figure 6. Double V Event as Seen on Film.

each event. We define a coordinate system on the stereographic pair of film negatives as shown in Figure 5, where the origins on the film are determined by the intersection of the optic axes of the lens with the film. Similarly we define a real space coordinate system, XYZ, whose origin is the intersection of the plane of the inner surface of the front glass (the XY plane) with the optic axis of the bottom camera lens. The Y-axis is in the upward direction parallel to the line of centers of the two lens, the X-axis is along the beam direction, and the Z-axis is perpendicular to the front window pointing into the chamber. Note that this is a left-handed coordinate system. The formulas relating a point on the stereo pair of film negatives (x, y, x', y') to a point in the real space of the bubble chamber (XYZ) are

$$X = x/v\,(S + Td + UZ),$$

$$Y = y/v\,(S + Td + UZ),$$

$$Z = \frac{2W - y/v(S + Td) - y'/v'(S' + T'd)}{y/vU + y'/v'U'},$$

where S and S' are respectively the distances from the bottom and top camera lens to the front glass window, v and v' are the distances from the two lens to the film, d is the thickness of the front glass window, and 2W is the distance between the optic axes of the two camera lens, Figure 5. In Figure 5 the X, Y, Z axes have been translated to the film plane to show their orientation relative to the xy and x'y' axes. The quantities T and U are

$$T(\alpha) = [n_1^2\,(\alpha^2 + 1) - \alpha^2]^{-\frac{1}{2}}$$

$$U(\alpha) = [n_2^2\,(\alpha^2 + 1) - \alpha^2]^{-\frac{1}{2}}$$

and $T' = T(\alpha')$, $U' = U(\alpha')$ where

$$\alpha^2 = \frac{x^2 + y^2}{v^2} \quad , \qquad \alpha'^2 = \frac{x'^2 + y'^2}{v'^2}$$

The quantities n_1 and n_2 are respectively the index of refraction of the glass and propane. These formulas are exact for a pin hole camera when lens aberrations are negligible and the film planes are parallel to each other and to the front glass window. Since α and α' are small quantities for our chamber (maximum value of about 1/3), T, T', U and U' are almost constant and to first order in α and α'

$$T(\alpha) = T'(\alpha') = 1/n_1 \quad ,$$

$$U(\alpha) = U'(\alpha') = 1/n_2 \quad .$$

We found that consistent with our measurement accuracy and the requirements of our experiment we could assume T and U constant and simplify the stereo formulas by introducing new "constants"

$$P = \frac{S + Td}{v} = \frac{S' + T'd}{v'} \quad ,$$

$$Q = \frac{U}{v} = \frac{U'}{v'} \quad .$$

After introducing three additional constants (G, x_o, y_o) to account for changing the origin to a convenient fiducial mark at the center of the front glass, the stereo formulas simplify to

$$X = x(P + QZ) + x_oQZ \quad ,$$

$$Y = y(P + QZ) + y_oQZ \quad ,$$

$$Z = \frac{-P(y + y')}{G + Q(y+y')} \quad ,$$

where the coordinates are now measured with respect to the new origin.

The constants P, Q and G are evaluated using the fiducial marks on the glass windows. These stereo formulas although approximate, proved to be completely adequate for our experiment.

3.3 Errors

The stereo formulas were used in an IBM 650 computer to calculate the real space coordinates of selected points on each event (Figure 6). It was expected that the calculated points would have an average error in X and Y of about 0.01 cm and in Z of about 0.01 cm. Repeated measurements confirmed this. From the selected points on each event the production (θ_{123}) and decay (θ_{234} and θ_{235}) angles, and the coplanarity angle between the line-of-flight of the neutral strange particle and the plane of the V were calculated. In addition the lengths of all line segments and the direction cosines of the ending pion beam track were calculated.

Since the production, decay and coplanarity angles were used to determine whether an event was real or not, it was important to know the expected angular errors in each event calculated. First of all by analyzing a large number of elastic scatterings it was determined that there was in general negligible systematic angular error. (For example, a systematic error in the stero formulas for some region of the chamber would cause a systematic angular error in that region.) To obtain an idea of the non-systematic angular errors involved in our experiment we note that an approximate angular error, $\delta\theta$, of production and decay angles is given by

$$\delta\theta \approx \left(\frac{1}{\ell_1^2} + \frac{1}{\ell_2^2}\right)^{1/2} \Delta \quad \text{radians},$$

where ℓ_1 and ℓ_2 are the track lengths of the two lines making the angle θ, and Δ is a suitable coordinate error (taken to be 0.1 cm). We see that for a short track length, less than one or two centimeters, the angular error can be very large. This is also true for coplanarity errors. Consequently, it was necessary to measure events that had short track lengths many times in order to obtain reliable angular information. After measuring numerous events we concluded that we could expect angular and coplanarity errors of about one degree after repeated measurements of short track length V^0's or if the track lengths involved were greater than 3 centimeters. Hence, for the indentification of events (Chapter IV), about one degree was taken as our basic angular acceptance region.

IV. IDENTIFICATION OF EVENTS

4.1 General Procedure

The identification of events was based primarily upon the production and decay process satisfying the relativistic kinematical relationships, i.e., the conservation of relativistic energy and momentum. We are concerned here with the identification of events where only one of the neutral strange particles produced decays in the chamber. In the production process the struck proton is one of the hydrogen atoms in propane and therefore is considered to be at rest. We define the laboratory production angle, as the angle between the incident pion and line-of-flight of the V°, i.e., the line between the ending pion track and the vertex of the decay V. Given the masses of the four particles, the incident pion energy and the production angle, the kinematical relations determine the momentum of the strange particle produced. Similarly given the decay angles (the angles between the line-of-flight and the two legs of the decay V) and the mass of the V°, the kinematical relations determine the momentum of the V° which decayed. For hydrogen events the production and decay momentum must be equal within error limits. The exception to this is those cases of $\Sigma^\circ - \theta^\circ$ hydrogen production where only the Λ° decays in the chamber. Since the Λ° is produced by the decay of the Σ°, its production momentum is not determined by the apparent production angle. Hence this class of events could not be distinguished from carbon production of V° particles.

The following general procedure was used in identifying all events.

1. Each event was first checked for coplanarity, i.e., the line-of-flight

of the V° must lie in the plane of the decay V within prescribed error limits. The error limits depended upon the length of tracks involved and the difficulty of the measurement, e.g., if part of the event was obscured by other tracks it sometimes was difficult to make accurate measurements. Since carbon V° events would also be coplanar, the coplanarity requirement only eliminated the extraneous background of V's. The extraneous V's were due to two pronged neutron stars from pion charge exchange scatterings in the propane and the neutron background at the Cosmotron, and to V° particles produced in the walls and windows of the chamber. Electron-positron pairs due to gamma ray conversion in the chamber also contributed to the V background. Of the over 500 V events measured, about 200 were coplanar within 3.5 degrees. The distribution of the coplanarity angle for hydrogen V° events is shown in Figure 7. Note the tremendous peaking of events for coplanarity angles less than one degree.

2. Those events which satisfied the coplanarity requirement were further analyzed on the basis of relativistic kinematical restrictions. Using the known masses of the particles involved, the pion beam energy of 1.1 Bev and conservation of relativistic energy and momentum, curves were drawn to give the momentum of the V° particles for all possible values of their production and decay angles. Each event was then successively assumed to be a Λ° from a Λ°-θ° production, a θ° from a Λ°-θ° production and a θ° from a Σ°-θ° production. (As was mentioned previously it was not possible to distinguish Λ°'s produced by decaying Σ°'s from carbon events.) For all three cases, the production momentum of the V° and the decay momentum

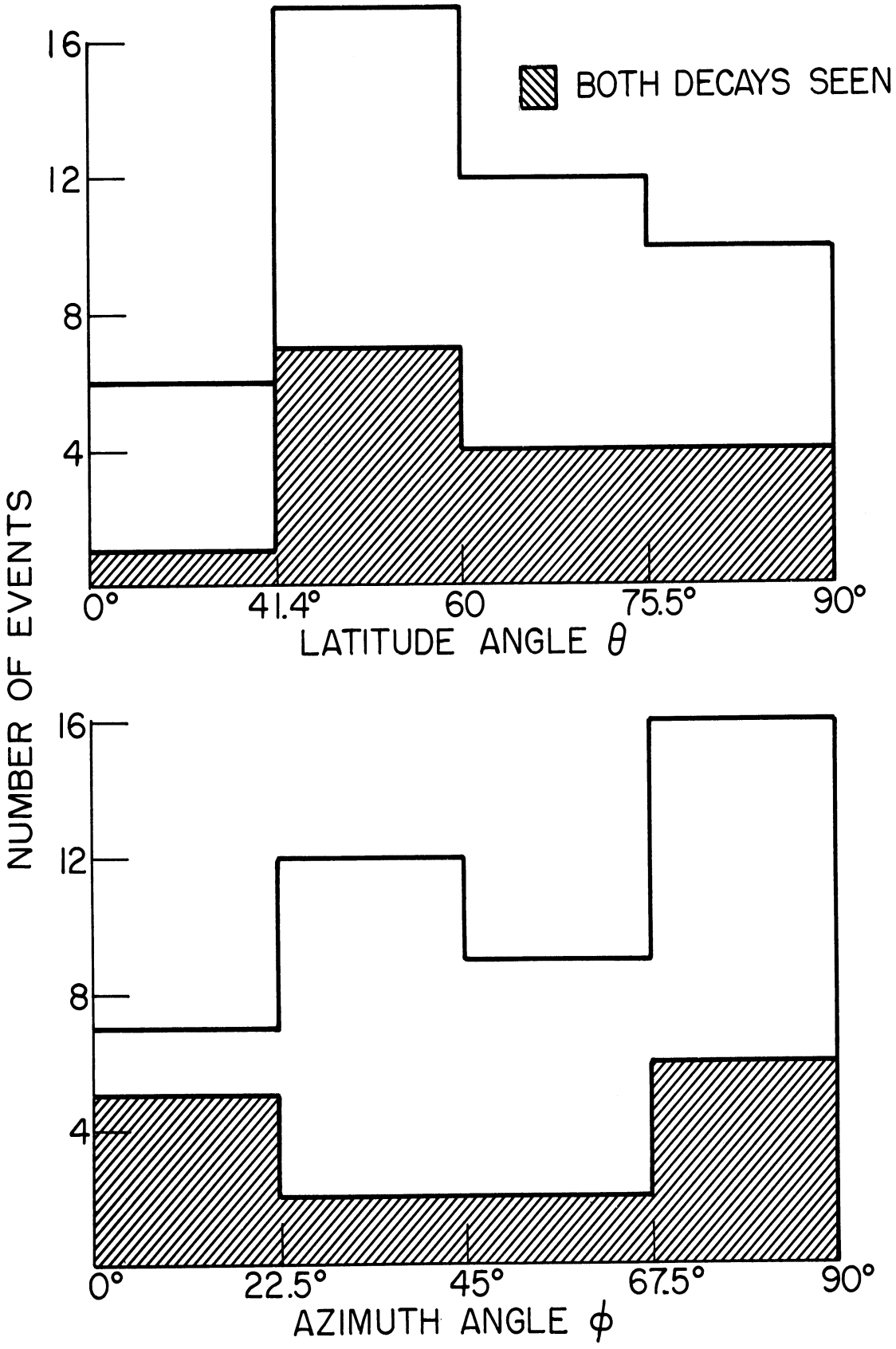

Figure 7. Distribution of Coplanarity Angle for V° Events.

of the V° were found and compared. If for any of the three cases the production and decay momenta were equal within prescribed limits, the event was classified as a possible hydrogen V° event. For each event the angular error limits had to be translated into momentum error limits before a comparison could be made. To satisfy the kinematical requirements an event had to have a production and decay momentum balance equivalent to about one degree angular error (Section 3.3). Events with high expected angular errors had to be measured many times before finally being accepted or rejected. All real events were measured at least twice.

3. The bubble densities of both secondaries from the decaying V° were then examined. It had been shown previously[10] that the bubble density of a particle track varies inversely as the square of its velocity. From the decay kinematics it was possible to calculate the velocity of the secondaries and thus check bubble densities. This criterion was used in only a qualitative way and bubble densities were classified as heavy, heavy medium, light medium and light. The standard was the incident (minimum ionizing) pion beam track which was classified as light. Those tracks with no bubble separation were classified heavy. As an aid in classifying bubble densities and to check on the validity of this requirement, we examined the bubble densities of the secondaries from a number of double V° events, i.e., events where both the Λ° and Θ° decay in the chamber. In these cases the kinematics are over determined and V° identification is positive. From these events we found that qualitative bubble densities could consistently be used to classify particle energies if account was taken of dipping tracks and the large bubble sizes of some tracks. Bubble

densities proved to be a useful method of distinguishing events which agreed kinematically as both Λ° and θ° events and for rejecting V's which accidently satisfied the kinematics for hydrogen V° events (Section 4.4). A total of 17 events which satisfied the kinematical requirements were rejected on the basis of bubble density.

4. Finally the ranges of both secondaries from the decaying V° were examined. The range of each secondary in propane is determined by its kinetic energy. For secondaries stopping in the chamber, the kinetic energy calculated from their range must agree with the kinetic energy calculated from the decay kinematics. For particles leaving the chamber, a check was made to see if their kinetic energy, calculated from the decay kinematics, was sufficient for this. A total of 7 events which satisfied the kinematical requirements were rejected on the basis of incorrect range. Some of these also had poor bubble density agreement.

4.2 Identification of Λ° Events

The identification of Λ° events proceeded as outlined above. In Figure 8 the Λ° production momentum is given in terms of its production angle, θ_Λ. The curves for a $\pm$ 5% change in pion beam momentum are also shown. Except for the tail of the curve, small errors in production angle or beam momentum change the production momentum very little. Hence the Λ° production momentum obtained from this curve is usually very reliable. The fact that the production momentum was a double valued function of the production angle caused little difficulty since bubble density alone was sufficient to distinguish between high and low momenta Λ° particles. However, the identification of Λ° particles whose decay angles were small

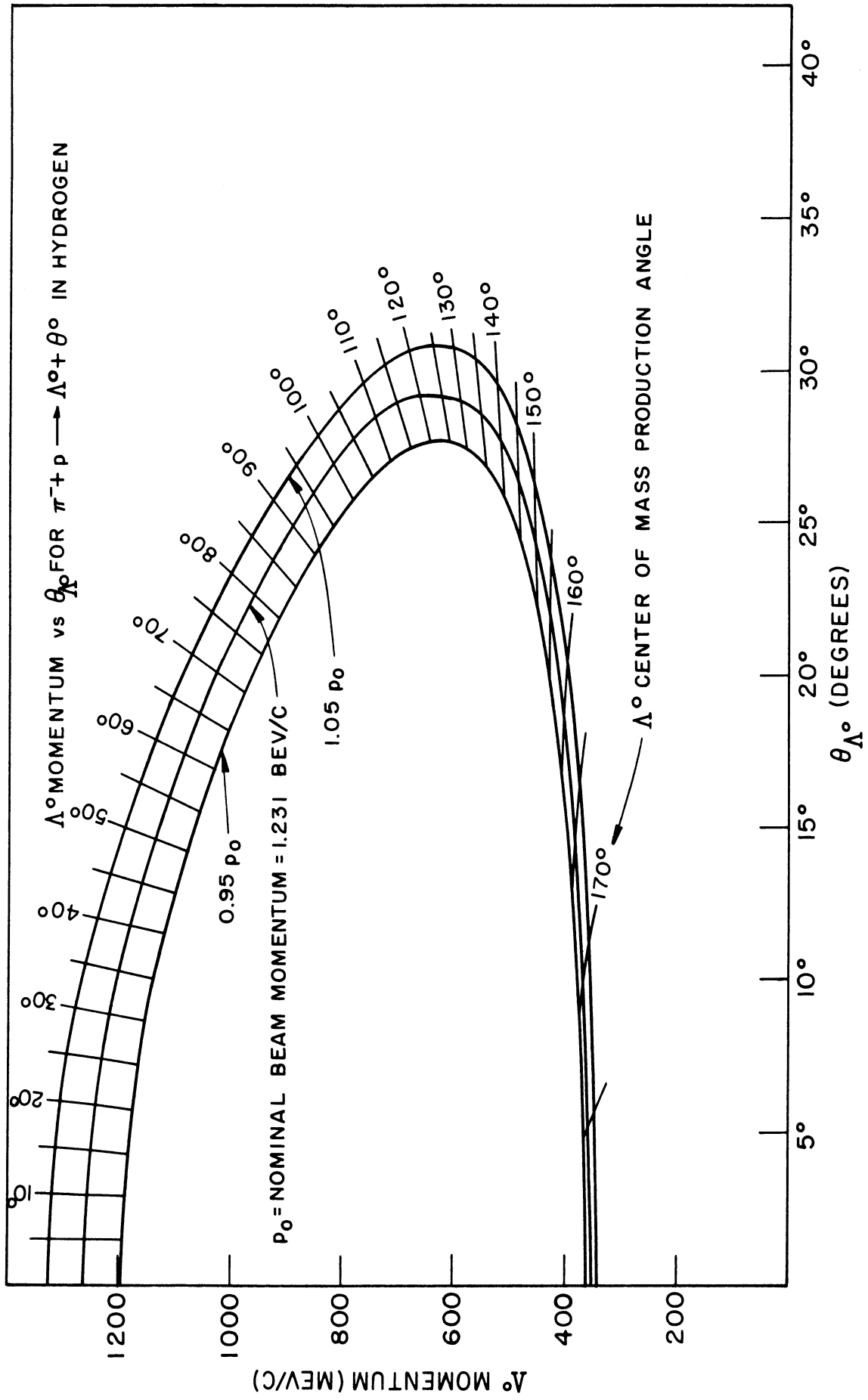

Figure 8. Momentum of Λ° vs. θ_Λ for Reaction $\pi^- + p \rightarrow \Lambda^\circ + \theta^\circ$.

presented some difficulty. In Figure 9 the Λ° decay momentum is given in terms of the decay angles. For small decay angles and high momenta Λ° particles, angular errors as small one or two degrees cause large momentum errors. In this region where decay momentum was such a sensitive function of decay angles, events had to be measured many times before finally being accepted. Also small decay angle Λ°'s could sometimes be confused with high energy electron-positron pairs.

There were 29 cases identified as $\pi^- + p \rightarrow \Lambda^\circ + \theta^\circ$ where the Λ° decayed in the chamber. In three of these cases, the secondary proton stopped in the chamber and in two of these cases the secondary pion stopped in the chamber and did not decay. Since the stopping of a secondary in the chamber over determines the kinematics, identification of these events can be considered positive. In the remaining cases both secondaries escaped and identification of these events was based on the kinematics and bubble density.

Two other cases of single Λ° decays were identified but upon re-scanning all the single Λ° events, an associated θ° was found for two events. The re-scanning was simplified since once a single Λ° event is identified, the line-of-flight of the associated missing θ° is determined. Hence all identified events (both Λ° and θ°) could be re-scanned along the expected line-of-flight for the associated V° with practically 100% efficiency.

4.3 Identification of θ° Events

There are two categories of single θ° events, those produced with an associated Λ° and those produced with an associated Σ°. The

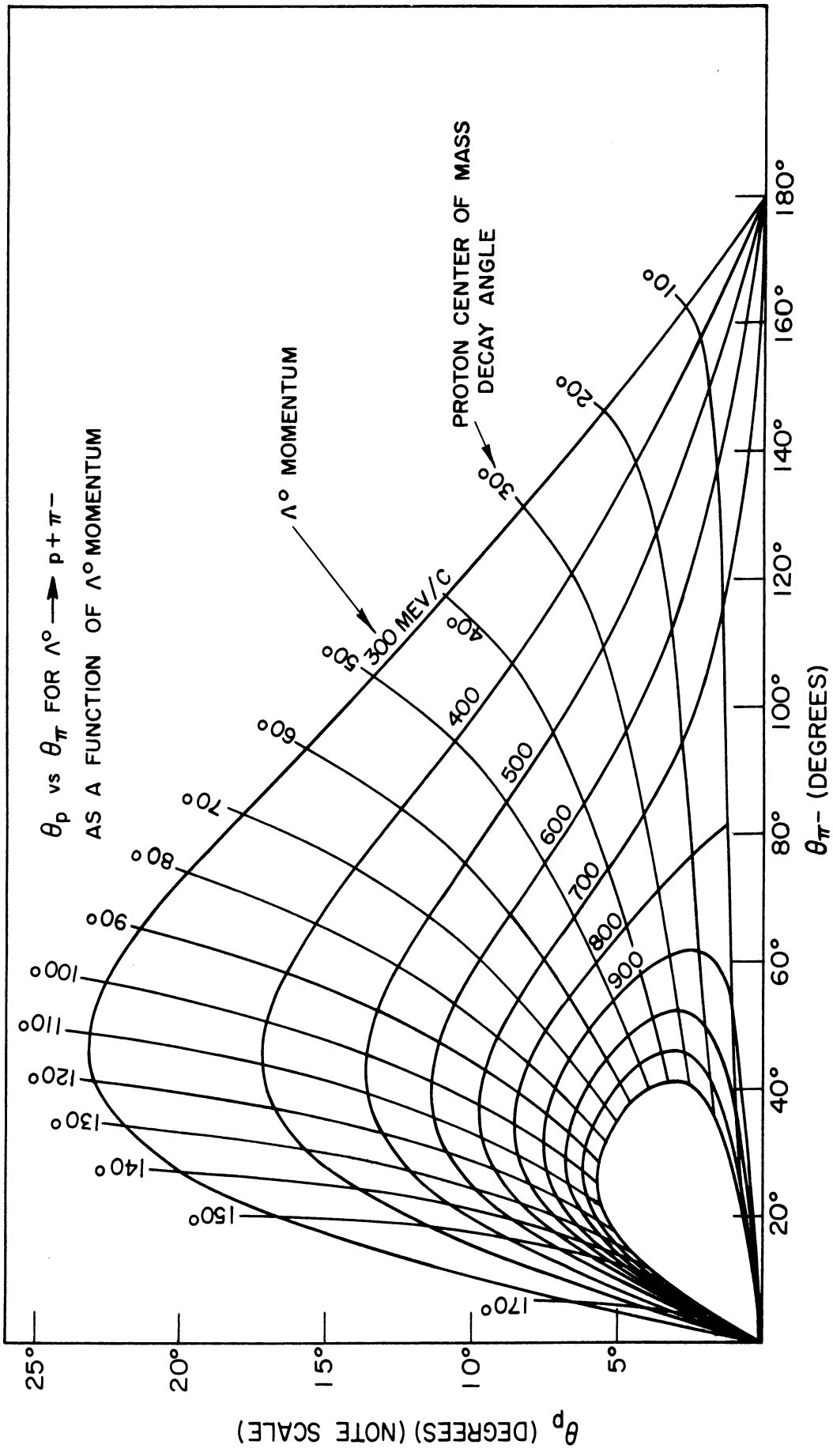

Figure 9. Graph of Θ_p vs. Θ_π for Λ° Decay.

production kinematics are different for these two categories since the mass of the Λ° and Σ° are different. For the most part, θ° production momenta obtained from production angles are quite reliable, since small changes in production angle and beam momentum cause only small changes in production momentum (Figures 10 and 11). As in the case of Λ° decay, the θ° decay momentum is more sensitive to small angular errors than the production momentum (Figure 12). However, there are no highly sensitive regions and in general the θ° events were easier to identify than the Λ° events.

There were 19 cases identified as $\pi^- + p \rightarrow \Lambda^\circ + \theta^\circ$, and 11 cases identified as $\pi^- + p \rightarrow \Sigma^\circ + \theta^\circ$, where in all cases only the θ° decayed in the chamber. There were three events where the secondary π^- meson stopped in the chamber and two events where the secondary π^+ meson stopped in the chamber and the identification of these events can be considered positive. There was one case where the γ-ray from the Σ° decay converted into an electron-positron pair in the chamber.

4.4 Carbon Contamination

Since the propane in the chamber is composed of both hydrogen and carbon (C_3H_8) it is possible that some of the V° productions identified as hydrogen events could have been produced on carbon protons. A kinematical study of this possibility indicated that the primary contribution of false hydrogen events would come from carbon protons of low Fermi momentum since these could kinematically agree, within measurement error, with hydrogen events. To estimate the number of such events we have examined all V events found by the scanners which were coplanar within 3° with the "line-of-flight"

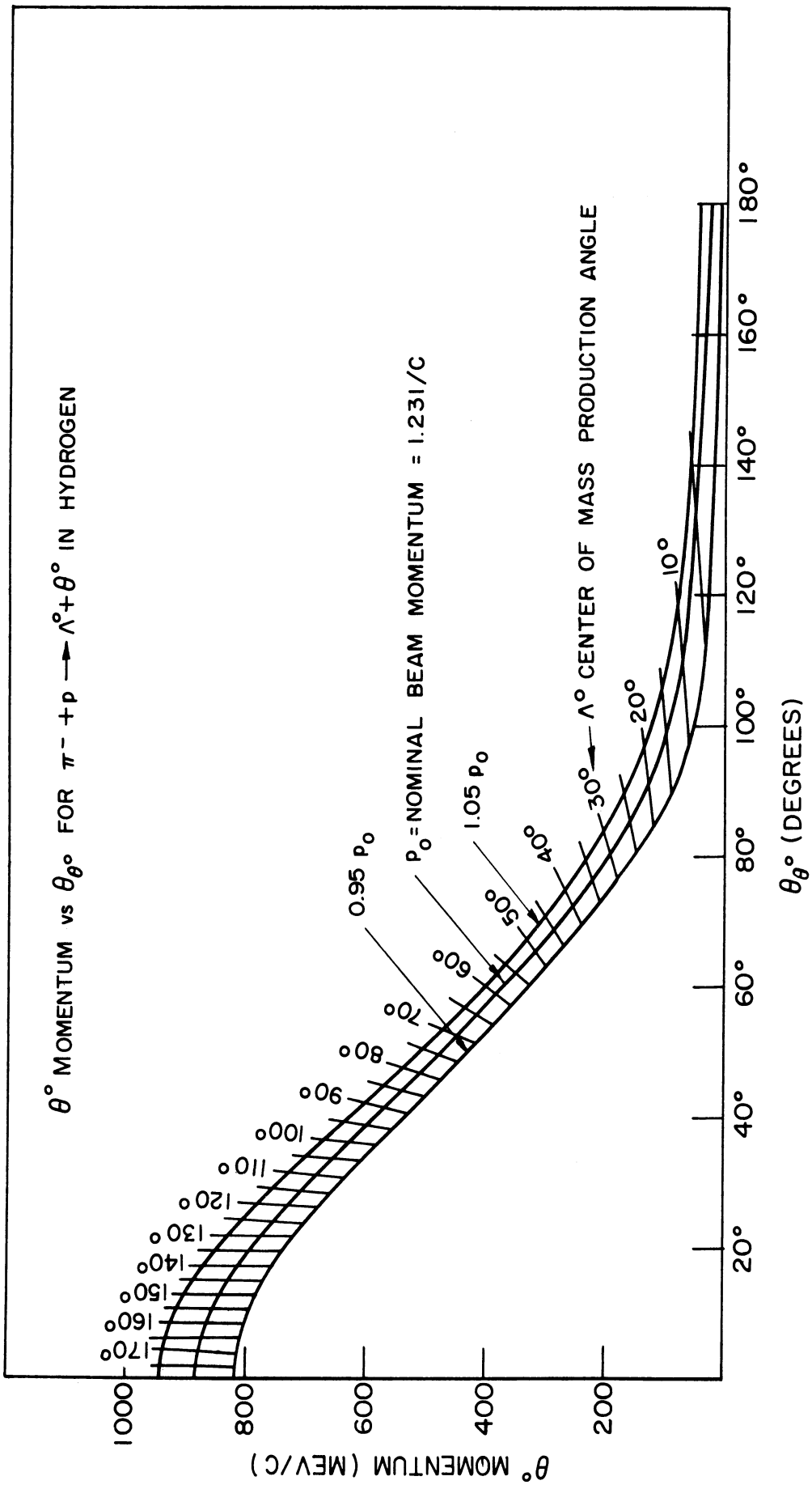

Figure 10. Momentum of θ° vs. θ_θ for Reaction $\pi^- + p \rightarrow \Lambda^\circ + \theta^\circ$.

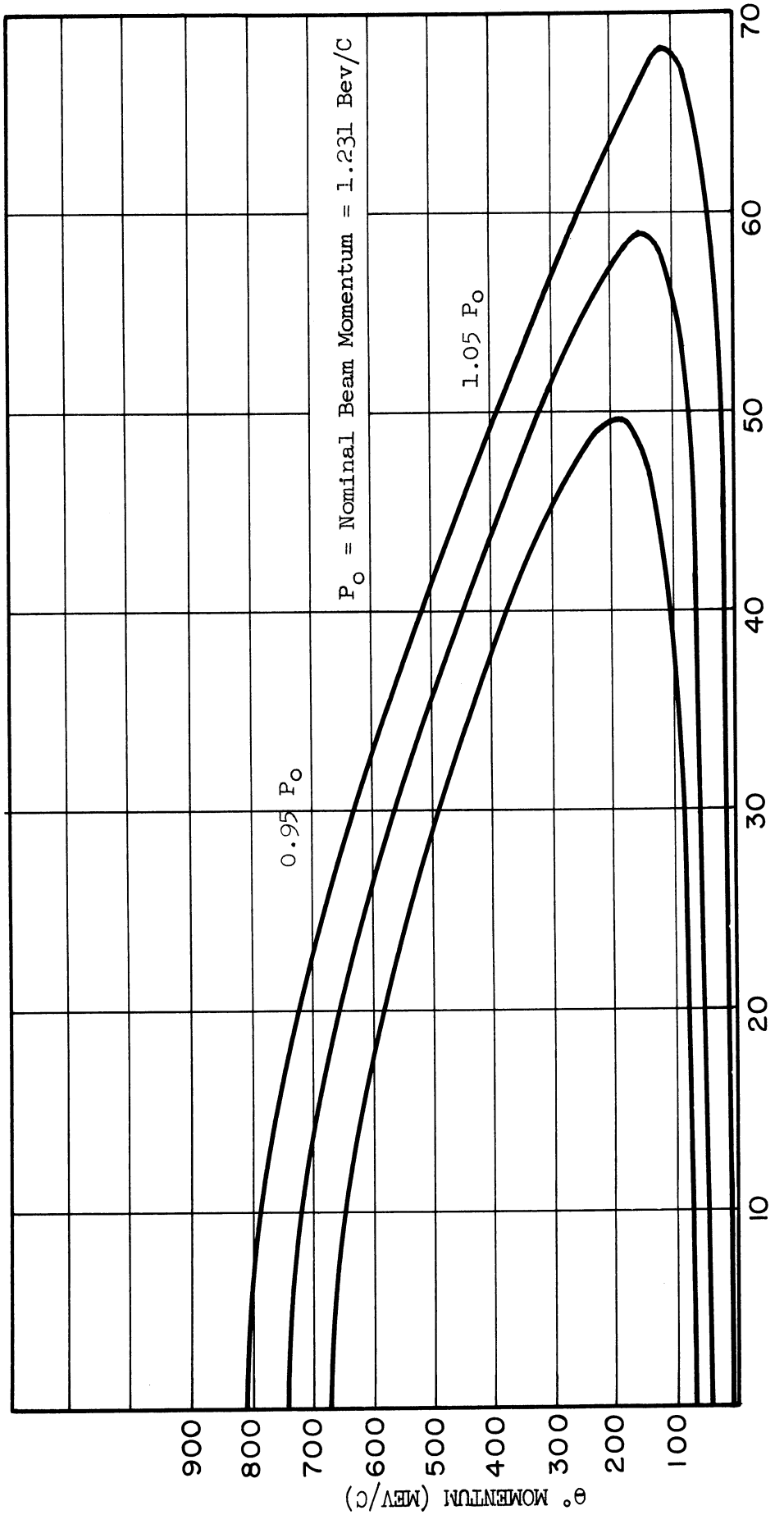

Figure 11. Momentum of θ° vs. θ_θ for Reaction $\pi^- + p \rightarrow \Sigma^\circ + \theta^\circ$

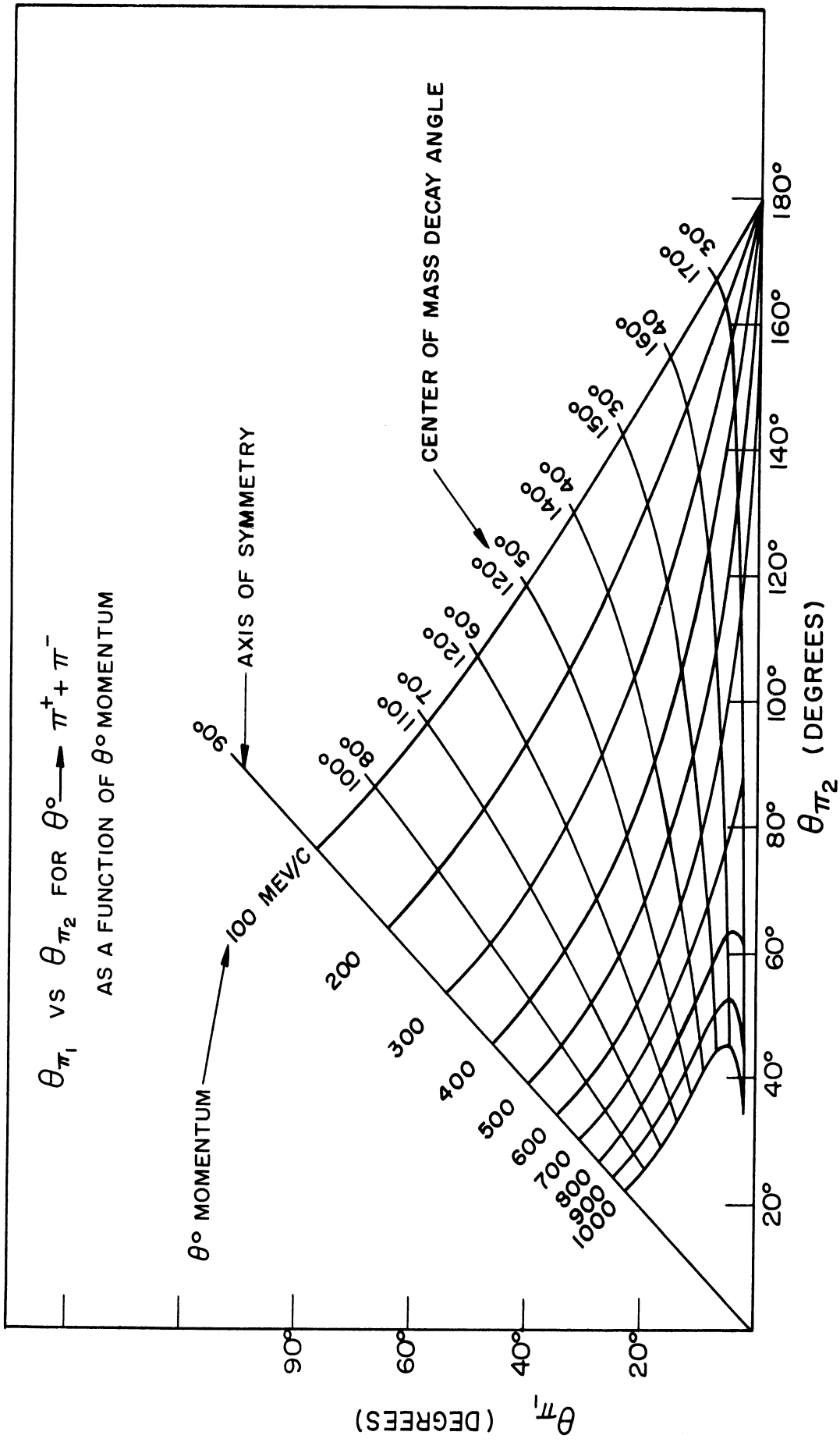

Figure 12 Graph of $\theta_{\pi 1}$ vs. $\theta_{\pi 2}$ for $\theta°$ Decay.

from a prongless ending pion beam track. The non-coplanarity of real hydrogen events was always less than this (Figure 7), but frequently only after the average of a number of measurements were taken and the carbon V°'s generally have been measured only once. There was a total of almost 200 coplanar V's, about half of them real hydrogen events and the remainder formed the background of carbon V°'s. The background also contained hydrogen Σ°-θ° productions where only the Λ° from the Σ° decayed in the chamber since these events could not be distinguished from carbon events.

To determine the number of carbon V°'s erroneously identified as a hydrogen Λ° productions we have treated each background V as a possible hydrogen Λ° event. The production and decay angles and the hydrogen kinematical curves were used for each of the background events to determine a "production and decay momentum". Each such event then determined a point on a "production momentum" versus "decay momentum" plot. This plot is shown in Figure 13. The real hydrogen Λ° events (also shown in Figure 13) fall within a band of $\pm$ 100 mev/c about the 45° line, where the production momentum equals the decay momentum. Some events which fell within this band were rejected because of range and/or bubble density or because their angular disagreement was greater than that allowed by our acceptance criterion. (It must be remembered that hydrogen event identification was based upon kinematical angular agreement within one degree, and momentum errors are not a linear function of angular errors.) Since the background of events is a smoothly varying distribution, it is possible to estimate the number of carbon events

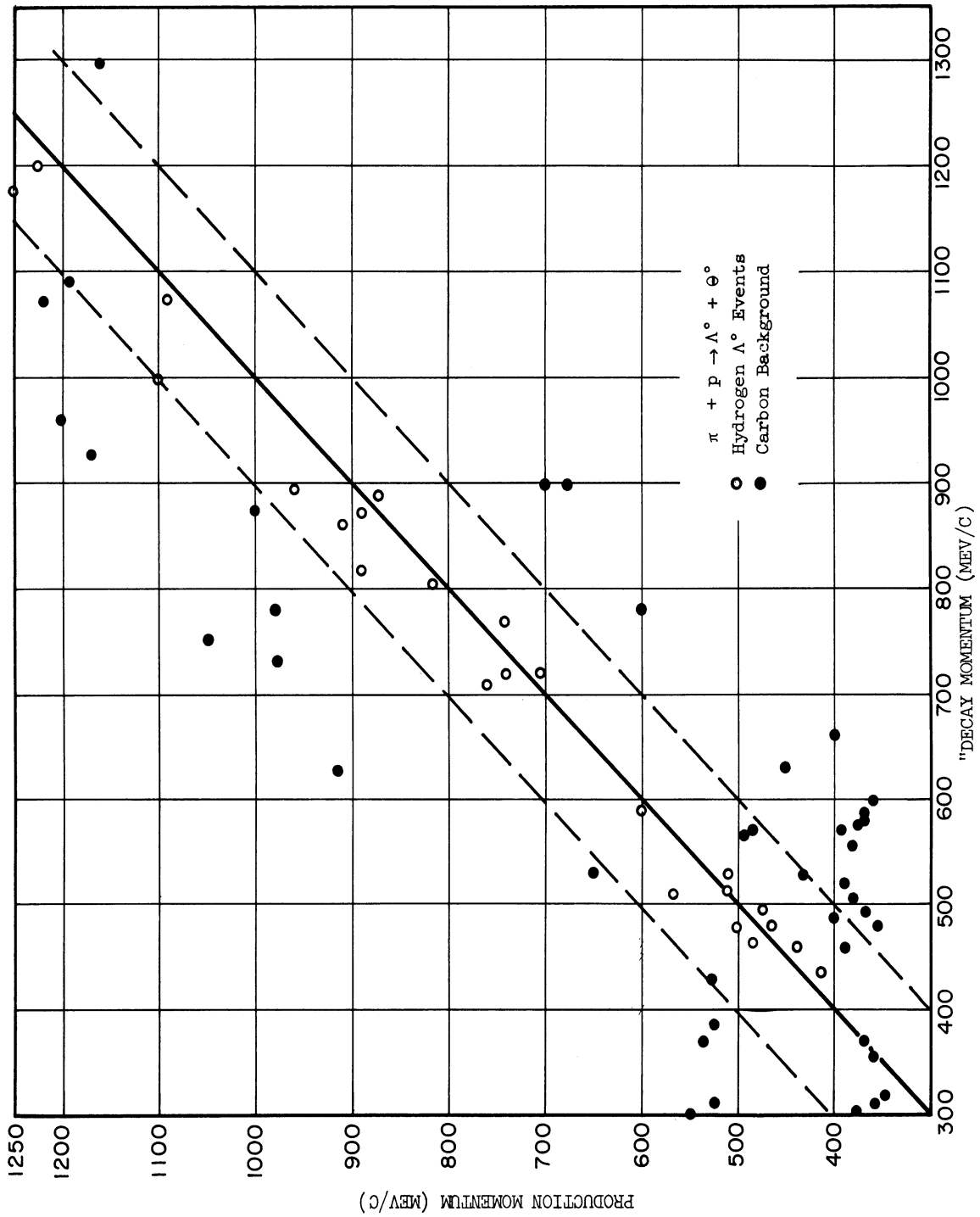

Figure 13. Distribution of Carbon Background and Hydrogen Λ° Events from Λ° - θ° Production.

contained in the hydrogen events acceptance region by examining the density of background points near this region. By extrapolation, we estimate (after subtracting background V's with poor bubble density or range), a carbon contamination in Λ°-θ° production of 23 $\pm$ 8% in the identification of single Λ° decays. Note that the density of background events approximately follows the density of hydrogen Λ° events, i.e., the momentum regions which contain a large number of Λ° events also contain a large carbon background. Hence it was not necessary to estimate different carbon contaminations for different Λ° momenta.

Similar plots were made for single θ° decays from Λ°-θ° productions (Figure 14) and Σ°-θ° productions (Figure 15). Again by extrapolation we estimate a carbon contamination in single θ° decays of 15 $\pm$ 8% for Λ°-θ° productions and 27 $\pm$ 15% for Σ°-θ° productions.

4.5 Scanning Efficiency

The total of about 31,000 pictures was scanned by three girls. To determine their efficiency for finding V° events, 1000 typical pictures previously scanned by one of the girls were selected for re-scanning by the other two girls.

The V's found by the scanners in the 1000 pictures can be divided into three categories: 1. V's that looked possible, i.e., that passed our fine scanning. 2. Only those V's which were coplanar with the line-of-flight. 3. Only those V's which turned out to be real hydrogen V° events. All three of these categories were considered for calculating scanning bias. The first category has the statistical advantage of having the greatest number of V events. It has the

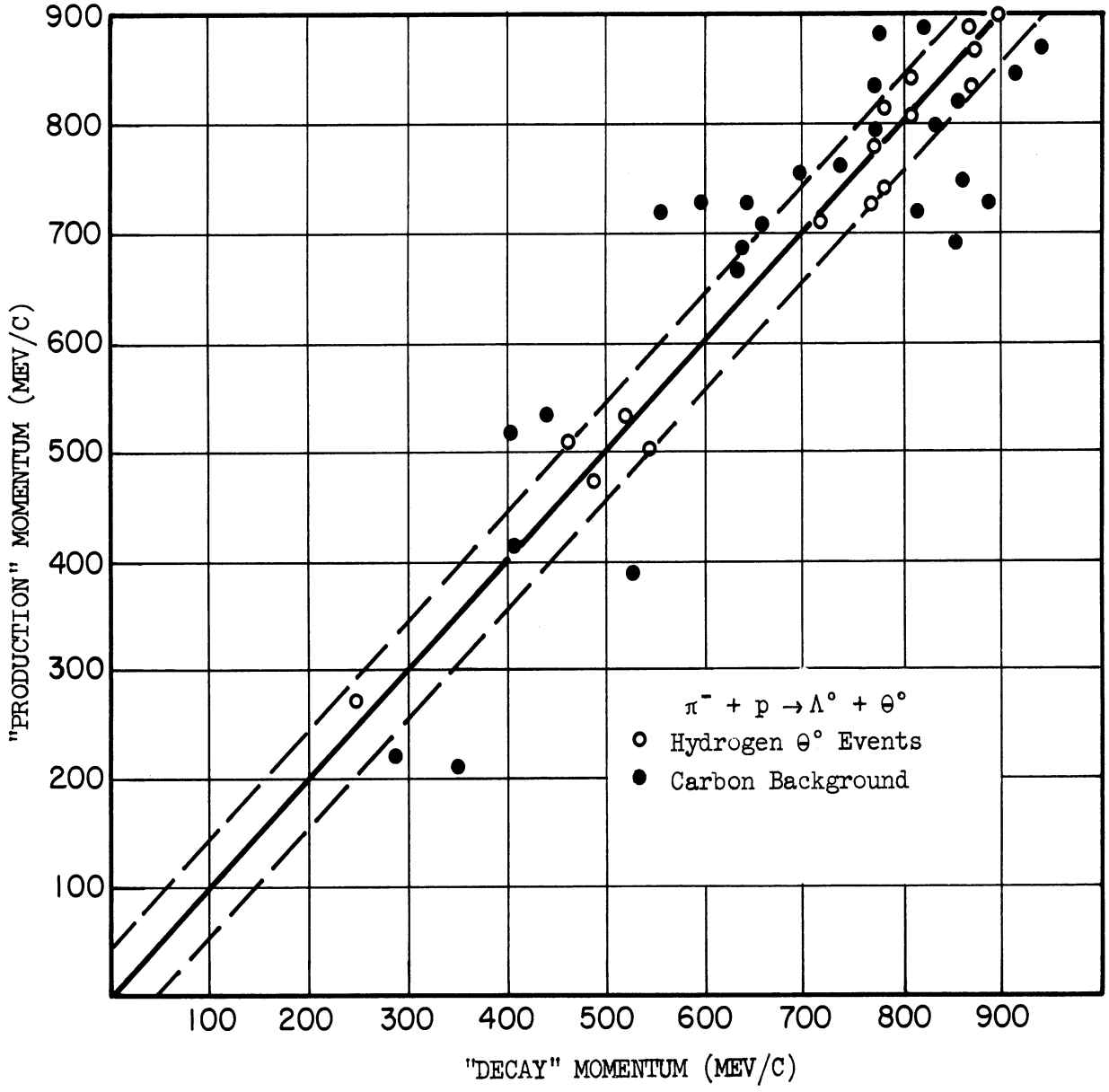

Figure 14. Distribution of Carbon Background and Hydrogen θ° Events from Λ°-θ° Production.

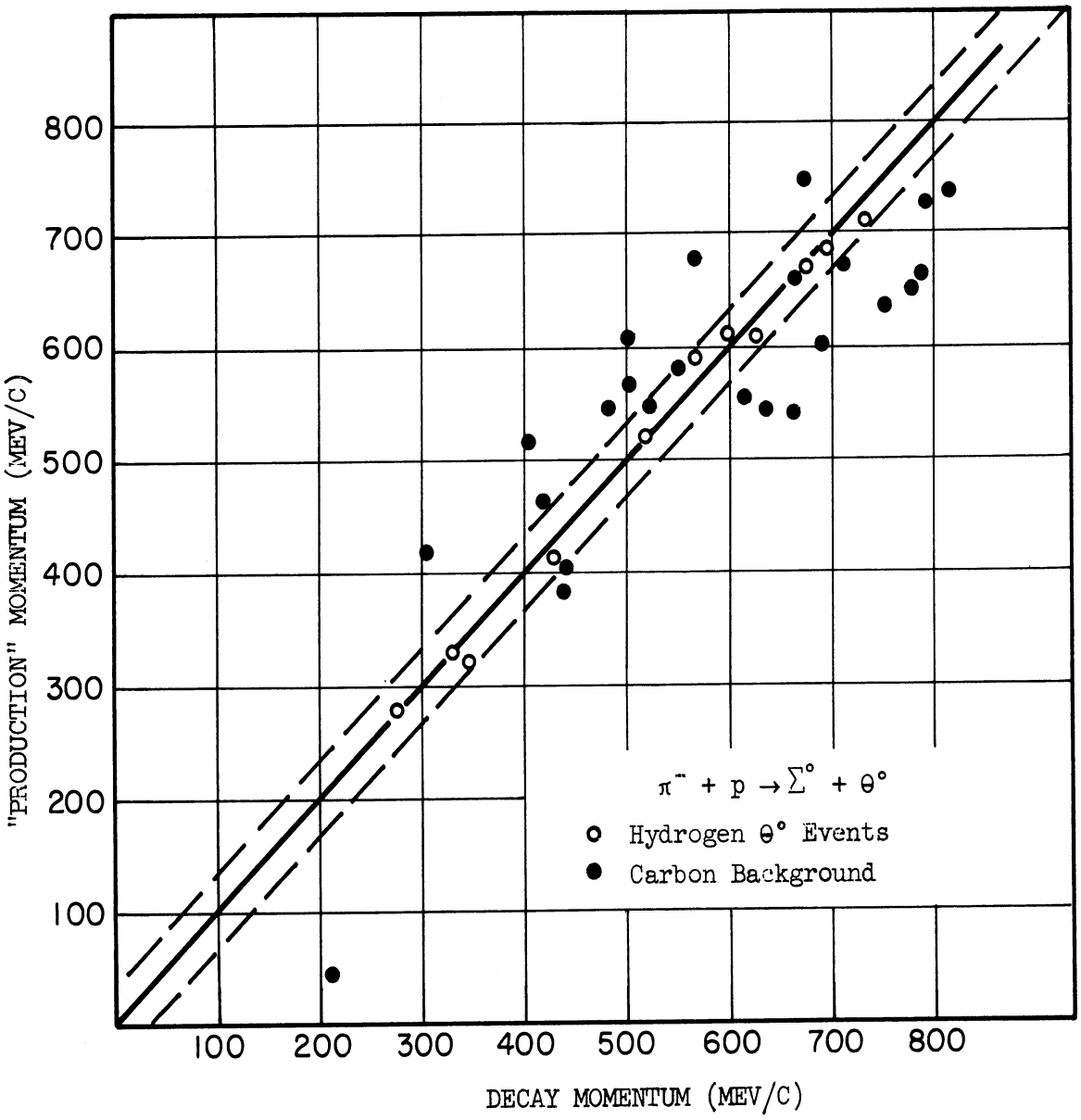

Figure 15. Distribution of Carbon Background and Hydrogen θ° Events from Σ°-θ° Production.

disadvantage of containing a large number of V's which are not V° events and thus could be a biased sample. It must be remembered that we are interested in the scanning efficiency for finding V° events, not V-shaped events. The second category has the advantage of containing almost solely V° events (although a large fraction of them are carbon V° events) and is still a large enough sample of events to be meaningful. The third category, while containing only hydrogen V° events, has the disadvantage of being a very small sample. Consequently, since we could conceive of no significant difference between the scanning efficiencies for carbon and hydrogen V° events, we chose the second category of events for calculating scanning efficiencies.

We designate the original scanner of the 1000 pictures by A and the two re-scanners by B and C. If n is the total number of coplanar events in the sample of pictures and T_A is the scanning efficiency of A, then the number of coplanar events that A finds (n'_A) is

$$n'_A = T_A n.$$

Similar expressions hold for scanners B and C. Also, we have the relations

$$n'_{ABC} = T_A T_B T_C n \quad ,$$

and

$$n'_{BC} = T_B T_C n \quad ,$$

for respectively the number of events that scanners A, B and C found in common (n'_{ABC}), and the number of events that scanners B and C found in common (n'_{BC}). Generally, scanning efficiencies are then found using

$$T_A = n'_{ABC}/n'_{BC} \quad ,$$

with similar expressions for T_B and T_C. The results obtained using these expressions are only correct under the following very restrictive conditions. 1. The scanning efficiency for all events is the same. This, of course, is not entirely correct. Some events are difficult to see and some are easy. This method does not take into account systematic scanning biases which discriminate against certain kinds of events. 2. The scanning efficiencies (T_B and T_C) of the re-scanners for this sample of pictures are typical of their scanning efficiencies in general.

Neither of these conditions was fulfilled in our experiment. It will be shown below that there were systematic scanning biases present. Further, although the re-scanners were instructed to scan the sample picture in their usual way, both of them markedly improved their scanning efficiencies for this sample. Actually one of them (who hates to be second best at anything) scanned all the pictures at 100% efficiency if the method given above were applied. This, of course, is absurd. Consequently, a new method of finding scanning efficiencies has been developed which gives correct results even though the second condition above is not satisfied, gives appreciably better statistics and is much less sensitive to systematic scanning biases.

First of all we show that correct relative scanning efficiencies can be found even though the above conditions are not satisfied. Consider all the pictures that hve been scanned, not just the re-scanned sample. Let N be the total number of pions entering the chamber and n the actual total number of events in the pictures. (Carbon events can also be used.) A certain fraction of the pictures have been scanned by A, another fraction

by B, and the remainder by C. For the fraction of pictures scanned by A, let N_A be the number of pions, n_A be the actual number of events, and n'_A be the number of events found by A. Let N_B, N_C, n'_B, etc. be defined in an analogous way. Then since

$$\frac{n_A}{n} = \frac{N_A}{N} \quad ,$$

and

$$n'_A = T_A n_A = \frac{T_A n N_A}{N} \quad ,$$

with similar expression for n'_B and n'_C, we have the following proportions which express the relative scanning efficiencies of A, B and C with known quantities:

$$T_A : T_B : T_C :: \frac{n'_A}{N_A} : \frac{n'_B}{N_B} : \frac{n'_C}{N_C} \quad .$$

The overall scanning efficiency, T, is just the weighted average:

$$T = \frac{N_A}{N} T_A + \frac{N_B}{N} T_B + \frac{N_C}{N} T_C \quad .$$

We can easily show that these expressions for relative scanning efficiencies are independent of systematic scanning bias. Suppose, for example, there were two classes of events with scanning efficiencies T_{A1}, T_{A2}, T_{B1}, T_{B2}, T_{C1}, T_{C2}. Then the number of events that A finds is

$$n'_A = n'_{A1} + n'_{A2} = T_{A1} n_{A1} + T_{A2} n_{A2} = T_A (n_{A1} + n_{A2})$$
$$= T_A n_A = \frac{T_A n N_A}{N} \quad ,$$

where now T_A is the weighted average of T_{A1} and T_{A2},

$$T_A = \frac{n_{A1}}{n_A} T_{A1} + \frac{n_{A2}}{n_A} T_{A2} \quad .$$

This expression can be generalized to include any number of systematic scanning efficiencies. Since similar relations hold for T_B and T_C, the expressions for relative scanning efficiencies are unchanged even when systematic scanning biases are present. Note also that since all of the pictures are included in this method, a statistically large sample is obtained. Hence, if we can determine the correct absolute scanning efficiency of one of the scanners from the re-scanned pictures, then the others can be found using the above proportions.

Consider now the sample of pictures originally scanned by A and re-scanned by B and C. Again suppose there are two classes of events with scanning efficiencies T_{A1}, T_{A2}, T_{B1}, etc., where T_B and T_C now refer to the efficiencies of B and C during the re-scan. If we define

$$f_1 = T_{B1}T_{C1},\ f_2 = T_{B2}T_{C2} \quad ,$$

then the expression used before to find T_A is now

$$\frac{n'_{ABC}}{n'_{BC}} = \frac{T_{A1}f_1n_1 + T_{A2}f_2n_2}{f_1n_1 + f_2n_2} \neq T_A \quad ,$$

i.e., in general this expression does not give T_A when scanning biases are present. Only under the exceptional circumstances that $f_1 = f_2$ does this expression give the correct value of T_A,

$$T_A = \frac{n_1}{n_1 + n_2} T_{A1} + \frac{n_2}{n_1 + n_2} T_{A2}$$

Hence, this method can give a serious error in the value obtained for T_A.

A much better way of obtaining a value for T_A is to instruct the scanners to re-scan the sample pictures very carefully, especially for

types of events suspected of being missed and then combine the results of the re-scanners to make them into a single scanner. Then the events found by A in common with B or C are used to calculate T_A. This has the effect of increasing the scanning efficiency for "hard" events proportionally more than for the "easy" events and makes the new values of f_1 and f_2 more nearly equal. For example, by combining the results of two re-scanners, B and C, f_1 and f_2 in the expression for T_A become the scanning efficiencies for the combined re-scanning (f_1' and f_2'), i.e.,

$$f_1' = T_{B1} + T_{C1} - T_{B1}T_{C1} \quad , \quad f_2' = T_{B2} + T_{C2} - T_{B2}T_{C2} \quad .$$

For cases of interest f_1' is approximately equal to f_2'. (Those kinds of events where the scanning efficiency is very low must always be treated separately, see below.) A typical example might be $T_{B1} = T_{C1} = 0.90$ and $T_{B2} = T_{C2} = 0.60$, then $f_1 = 0.81$ and $f_2 = 0.36$, in very poor agreement, while $f_1' = 0.97$ and $f_2' = 0.83$, in much better agreement. Remember that T_B and T_C are the re-scan efficiencies and should generally be considerably better than the original scanning efficiencies (see below).

Using this method, the absolute scanning efficiency of A was found to be $T_A = 0.71$. This result is independent of appreciable systematic scanning biases since one of the scanners re-scanned at essentially 100% efficiency. Using the proportions developed for relative scanning efficiencies we found $T_B = 0.80$ and $T_C = 0.55$. The weighted average of these three efficiencies gave for the overall scanning efficiency, $T = 0.68 \pm 0.10$.

4.6 Systematic Scanning Biases

The results of Section 4.5 include only those systematic biases which have appreciable scanning efficiencies, at least in re-scanning. Those kinds of events which have very small scanning efficiencies must be treated separately. We consider them here.

One systematic scanning bias appears to be introduced by the position of the event in the chamber. Histograms were made of the distribution in the chamber of about 150 coplanar events. The ending pion beam track and vertex of the V were used to define the position of an event and separate plots were made for each of these points. The distribution of events in chamber width and depth were uniform. However, the distribution of events along the length of the chamber had some unusual characteristics. In Figure 16 the distribution of the ending pion beam track versus its X position is shown. The chamber extends in length to X = $\pm$ 15 cm. and beam tracks enter at X = -15 cm. The missing events near the incident end of the chamber indicates that tracks near the ends of the chamber should be at least 3 cm. long to be seen with appreciable probability. This is a systematic bias which discriminates against those events which occur near the beginning of the chamber. The decrease in the number of events near the far end of the chamber is probably the superposition of a number of effects: 1. Scanning difficulty on short track length V's due to decays near the end of the chamber. 2. Events becoming obscured because of reflected light off the back window edges and frame, and by the increased background of tracks due to pion interactions with the propane. 3. Decay of V°'s outside of the end of the chamber. 4. Attenuation of the beam due to pion interactions

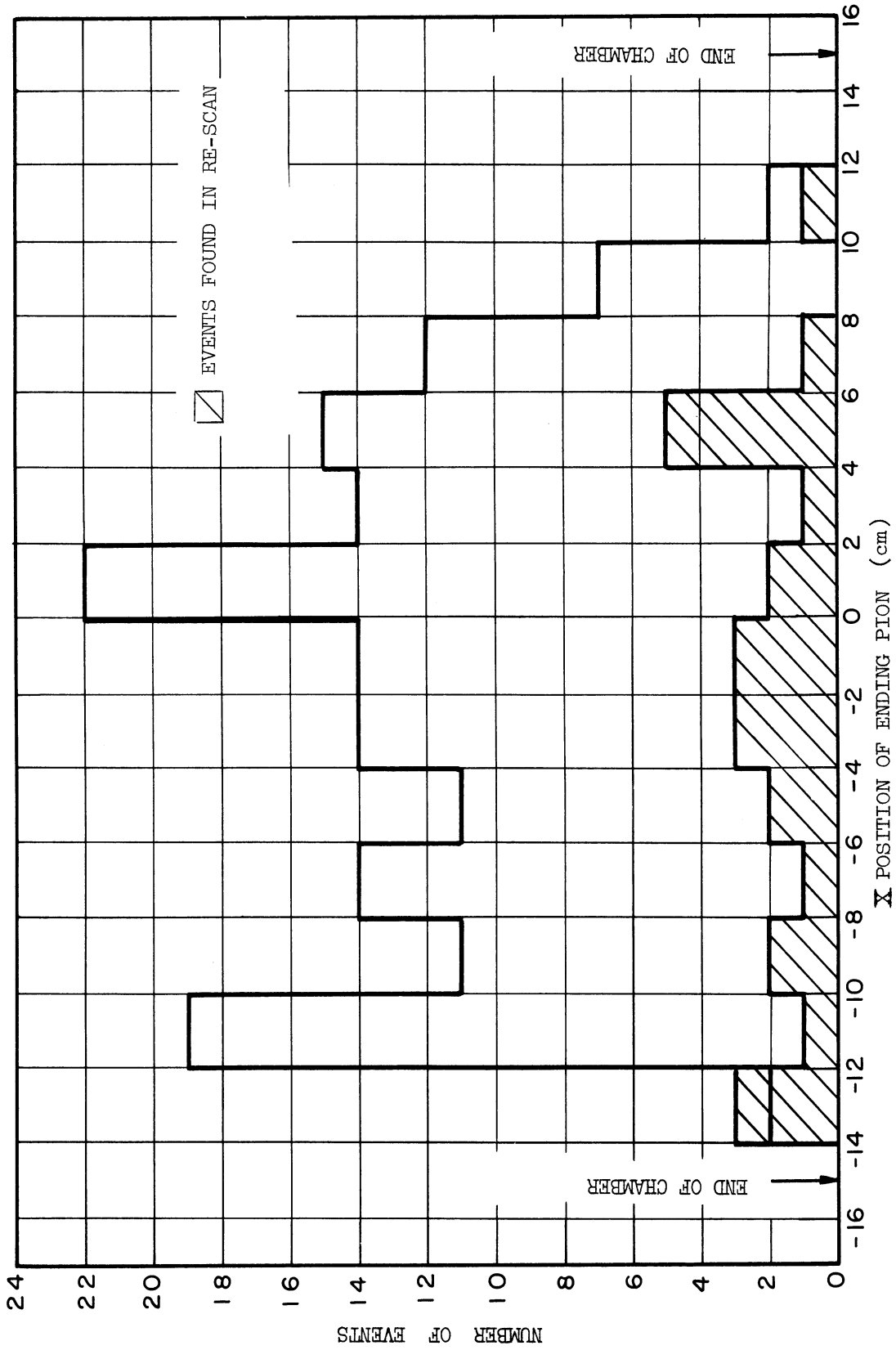

Figure 16. Distribution of Ending Pions in Bubble Chamber.

with the propane. The last two effects are treated separately (Chapter V). The first two effects certainly contribute to a systematic scanning bias.

In Figure 16 we also show the distribution of events found in the re-scanned pictures. It appears to be quite uniform in the region X = -14 cm. to X = + 12 cm., indicating that in the careful re-scan of pictures this systematic scanning bias has almost disappeared since the deficiency of events in the last three centimeters can be accounted for to sufficient accuracy by effects (3) and (4), above. Thus the scanning efficiency calculation of Section 4.5 is applicable to the region of the chamber between X = -14 cm. and X = +15 cm., and our chamber is considered to be only 29 cm. long when making cross section calculations.

For comparison, the scanning efficiency can be calculated for the region of the chamber between X = -14 cm. and X = +12 cm. using the uniform part of the distribution between X = -12 cm. and X = +8 cm. This leads to a scanning efficiency of 0.75 as compared to 0.68 calculated in Section 4.5. The closeness of agreement of these two results indicates that a major part of scanning inefficiency is due to the position of an event in the chamber.

Another possible systematic scanning bias could have been introduced by the decay of V°'s very close to their origin. These may appear to be a two pronged star or a scattering rather than an ending pion and a V. However, a histogram made of the distribution of "decay" lengths of fifty events indicated that this introduced negligible bias (Section 5.4).

V. EXPERIMENTAL RESULTS

5.1 The Production of V° Particles

A total of 91 V° events were found where in each case the struck proton was free (hydrogen events). Thirty-two of these are double V° events, most of which have been reported elsewhere[8]. Since they are necessary for our analysis we include them here. Specifically we found:

1. 29 cases of $\pi^- + p \rightarrow \Lambda^\circ + \theta^\circ$ where the Λ° decayed in the chamber,
2. 19 cases of $\pi^- + p \rightarrow \Lambda^\circ + \theta^\circ$ where the θ° decayed in the chamber,
3. 11 cases of $\pi^- + p \rightarrow \Sigma^\circ + \theta^\circ$ where the θ° decayed in the chamber,
4. 17 cases of $\pi^- + p \rightarrow \Lambda^\circ + \theta^\circ$ where both the Λ° and θ° decayed in the chamber,
5. 15 cases of $\pi^- + p \rightarrow \Sigma^\circ + \theta^\circ$ where both the Λ° and θ° decayed in the chamber.

As mentioned previously, it was not possible to distinguish $\pi^- + p \rightarrow \Sigma^\circ + \theta^\circ$ hydrogen reactions from carbon reactions when only the Λ° decayed in the chamber since the intermediate decay of $\Sigma^\circ \rightarrow \Lambda^\circ + \gamma$ made it impossible to assign an unambiguous production momentum to the Λ°. In the Appendix a list of all the events, with their production and decay angles is given.

To calculate the total cross sections for $\Lambda^\circ - \theta^\circ$ and $\Sigma^\circ - \theta^\circ$ productions on free protons from the above data a number of factors must

be considered. The two quantities "measured" in this experiment which go into the cross sections are the number of events and the number of pion beam tracks. We consider first corrections that must be applied to the number of events.

1. Approximately 75% of our pictures were of uniform quality and we use only these in calculating cross sections. We considered the other 25% of our pictures to be of lower quality because the bubble sizes are small enough to make scanning difficult. In the pictures of uniform quality we found from Λ° - θ° productions, 26 single Λ° events, 17 single θ° events and 15 double Λ° - θ° events; from Σ° - θ° productions, we found 11 single θ° events and 14 double Σ° - θ° events.

2. In Section 4.4 we estimated a carbon contamination in Λ° - θ° production of about 23% in the identification of single Λ° events and 15% in the identification of single θ° events. For Σ° - θ° production we estimated a carbon contamination of about 27% in the identification of single θ° events. In reference 8 the carbon contamination in double V° events was estimated to be about 6% for double Λ° - θ° events and about 25% for double Σ° - θ° events.

3. In Section 4.5 we estimated a scanning efficiency of 68% for finding single V° events. A scanning efficiency of about 80% was estimated for finding double V° events[8].

4. In Chapter IV we noted that their had been some experimental and theoretical evidence indicating the existence of neutral and long lived V^e decay modes. In Section 5.4 it will be shown that our data (as well as data from other experiments similar to ours) does indeed indicate that an appreciable fraction of V° particles decay be either a long lived or neutral mode. Since these types of V° events will not be seen in our chamber, it is necessary to take account of them when calculating total cross sections. Consider only the pictures of uniform quality and let $N_{\Lambda\theta}$, N_Λ and N_θ be respectively the number of events after correction for scanning bias and carbon contamination where both the Λ° and θ° decayed in the chamber, where only the Λ° decayed in the chamber, and where only the θ° decayed in the chamber. Also let $P_{\Lambda\theta}$ be the probability of Λ° - θ° production by the interaction of a pion with a free proton, N_π be the number of pion tracks, α_Λ and α_θ be respectively the probabilities that the Λ° and θ° decay by their normal lived charged mode, and finally let P be the probability that a V°, decaying by its normal charged mode, decays before leaving the chamber. With these definitions we have

$$P_{\Lambda\theta} = \frac{N_{\Lambda\theta}}{N_\pi \alpha_\Lambda \alpha_\theta P^2}$$

To show the explicit dependence of $P_{\Lambda\theta}$ on the number of single

V° events, we substitute the formulas for α_Λ and α_θ developed in Section 5.4 and obtain

$$P_{\Lambda\theta} = \frac{N_{\Lambda\theta} + N_\Lambda + N_\theta + \frac{N_\Lambda N_\theta}{N_{\Lambda\theta}}}{N_\pi}$$

The cross section for Λ° - θ° production by pions on free protons is then

$$\sigma(\Lambda\theta) = \frac{P_{\Lambda\theta}}{WL}$$

where W is the density of free protons (hydrogen atoms) and L is the length of the chamber. A similar expression holds for Σ° - θ° production.

We next consider the corrections applied to the total length of pion track, $N_\pi L$. To determine the number of pions entering the chamber the scanners counted beam tracks on every tenth picture. To this number we applied the following corrections:

1. From data taken with counters during an experiment using a meson beam similar to ours[11,12], we estimate a μ^- meson and electron contamination in our beam of about 8%. This number was substantiated by examining about 200 pictures for beam particle interactions of any kind in the liquid. This determines the total beam interaction cross section. Since the total pion cross section for carbon and hydrogen at this energy is known[12] an estimate can be made of the μ^- meson and electron contamination of the beam by comparing the two values.

2. From the published data on meson total cross sections with protons and carbon at this energy[12], we applied a beam attenuation factor of about 12% due to non-strange particle π^- meson interactions in the liquid.

3. Because of the finite width of our collimators and meson scattering off the shielding, magnet pole pieces, etc., we expected that a fraction of the pions entering the chamber would appear to the scanners to be beam particles but would have the wrong momentum. As long as the indicent pion angle with respect to the chamber was not large enough to be detectable by eye, the pions would be counted as beam particles. Since the V° events produced by "off beam" pions would not kinematically check out as real events, a low value of the cross section is obtained by counting them as beam particles. To correct for this, a histogram was made of the distribution of the direction cosine with respect to the Y-axis of 117 tracks which appeared to be beam tracks (Figure 17). With respect to the (X,Y,Z) coordinate system defined in Section 3.2, a "perfect" beam particle would have direction cosines of (1,0,0). The distribution is approximately normal, with about 19% of the pions having their direction cosine outside the interval $\pm$ 0.012. Also shown in Figure 17 is the distribution of 117 pions which caused hydrogen V° events. This distribution is appreciably narrower, with only about 6% of the pions having their direction cosine outside the interval $\pm$ 0.012. Taking

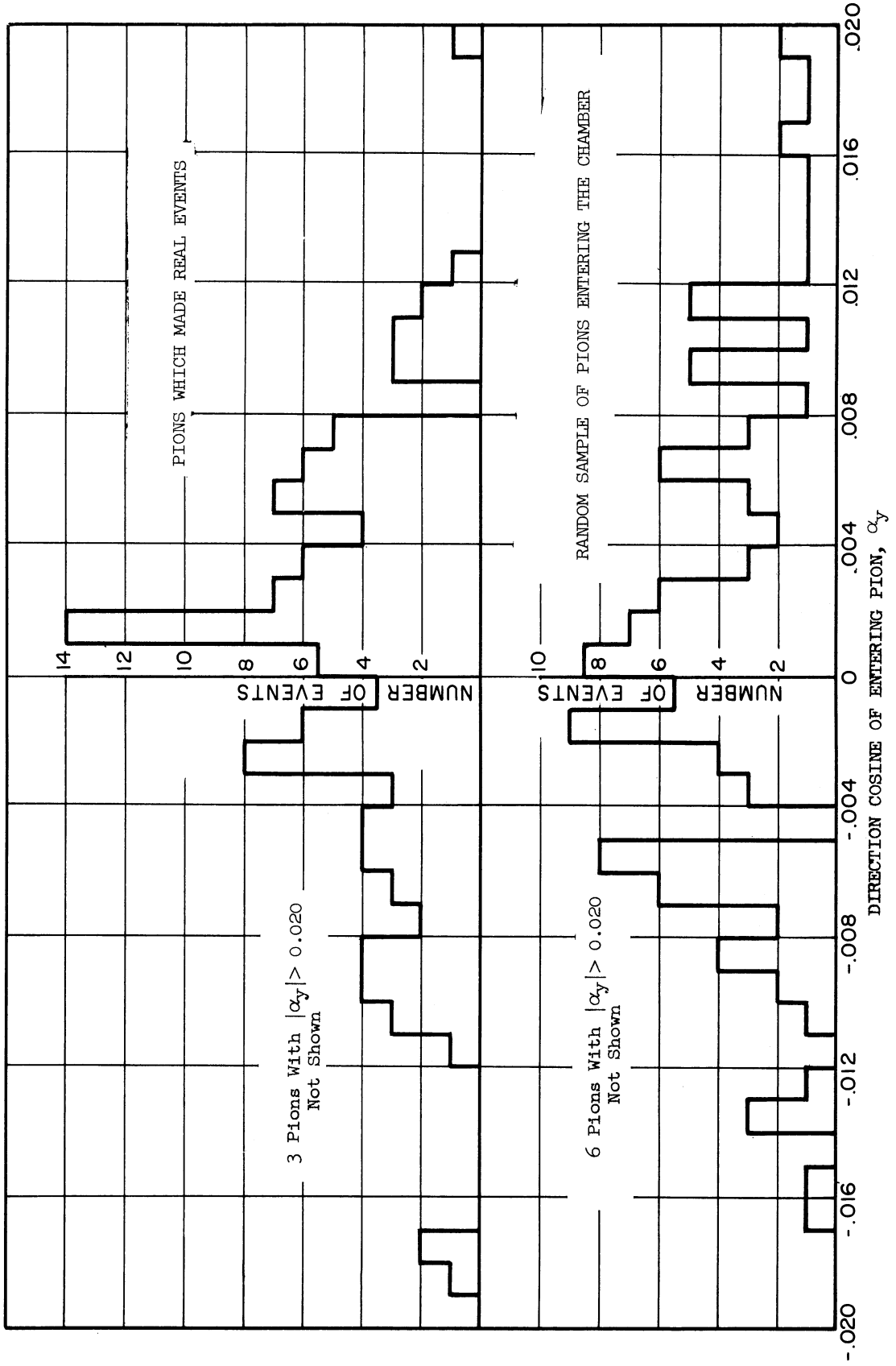

Figure 17. Distribution of Entering Pions.

into account the μ^- mesons and electrons contained in the former distribution, we estimate that about 11% of the pion tracks counted were not beam tracks.

4. In Section 4.6 we noted that the scanning efficiency for beam tracks less than 1 cm. long was essentially zero. Consequently we used a chamber length of 29 cm. (instead of 30 cm.) when calculating the total length of pion track.

After applying these corrections we found the following values in millibarns for total cross sections for producing ($\Lambda^\circ\theta^\circ$) particles and ($\Sigma^\circ\theta^\circ$) particles by 1.1 Bev π^- mesons on free protons,

$$\sigma_{\Lambda\theta} = 0.28 \pm 0.04 \text{ mb.},$$

$$\sigma_{\Sigma\theta} = 0.16 \pm 0.04 \text{ mb.}$$

The errors are standard deviations. They are primarily due to the uncertainty in the number of events because of statistical fluctuations in a sample of this size, and the uncertainty in the values of scanning efficiency and carbon contamination.

In Figure 18 the angular distribution of the hyperons (Λ° or Σ°) in the center-of-mass system of production is shown. For comparison the angular distribution of the Σ^- and Σ^+ hyperons produced at the same pion energy are also given[8,11]. The Λ° distribution has a pronounced peak in the backward hemisphere. The Σ° hyperon also tends to go off in the backward hemisphere but is less peaked than the Λ° distribution. In contrast, the Σ^- and Σ^+ distributions are peaked in the forward hemisphere. Comparison of the Σ hyperon production angular distributions using the

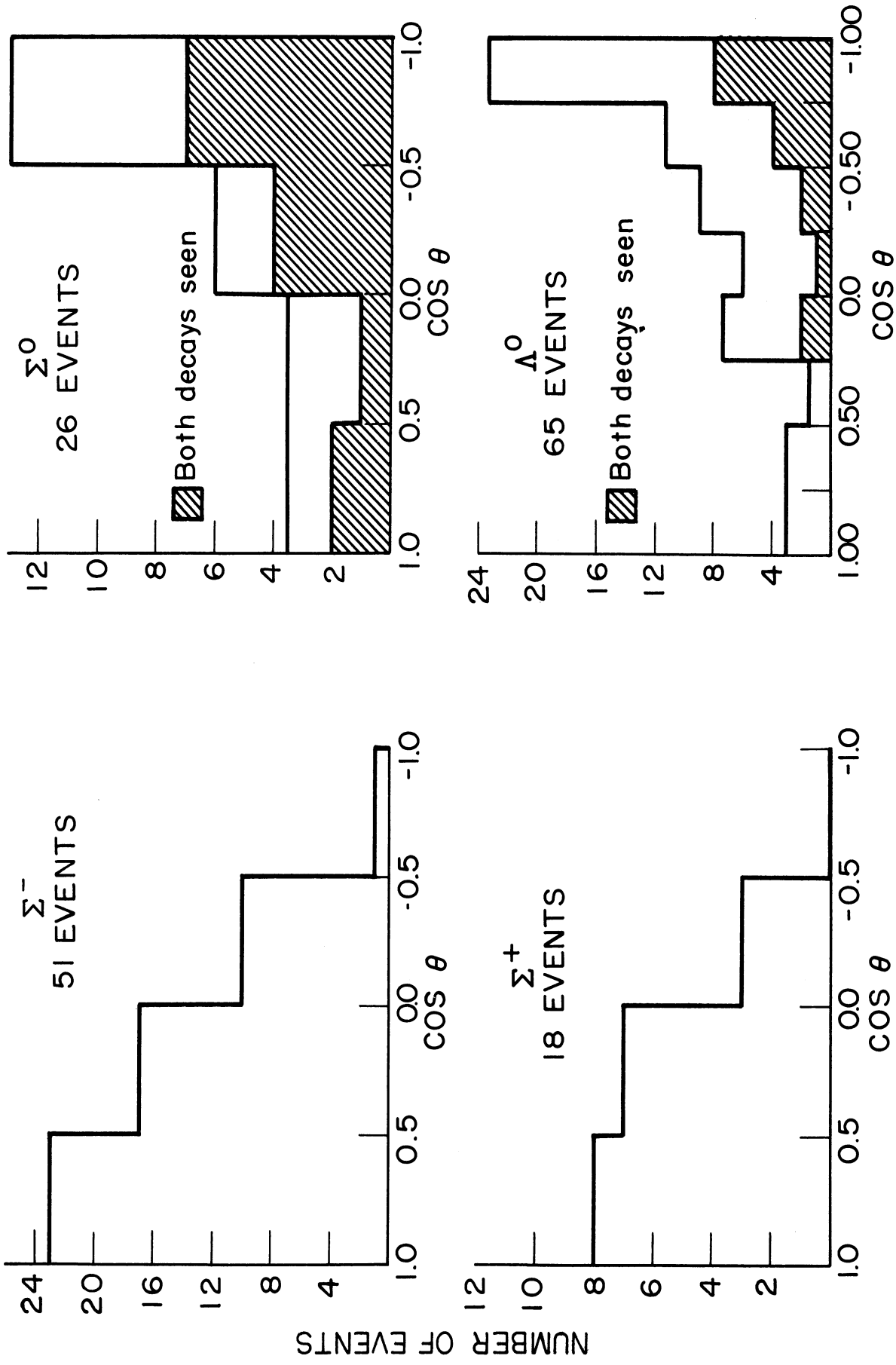

Figure 18. Hyperon Production Center of Mass Angles.

results of references 8 and 11 seemed to contradict the hypothesis of charge independence in the production process[13]. However, the addition of the Σ° events given here indicates that the magnitude of the discrepancy is not as great as was given previously[11].

5.2 The Decay of V° Particles

It has been pointed out by Lee et al.[14], Morpurgo[15], Adair[16], and others that an examination of the angular distributions of the decay of V° particles may yield information on their intrinsic parities and spins. To examine these angular distributions we use a coordinate system, defined in the rest system of the decaying particle, which is the same as used by Morpugo[15] and is shown in Figure 19. The latitude angle θ $(0 \leq \theta \leq \pi)$ and the azimuthal angle φ $(0 \leq \varphi \leq 2\pi)$ are the center-of-mass angles of the π^- in the Λ° decay. However, for the Θ° decay the latitude angle θ $(0 \leq \theta \leq \pi/2)$ and the azimuthal angle φ $(0 \leq \varphi \leq \pi)$ are the center-of-mass angles of either π meson, since in general we cannot tell them apart. Note that the angle φ gives the angle between the production and decay planes. In Figures 20 through 22 the angular distributions of decay, $I(\theta)$ and $I(\varphi)$ are plotted for both the Λ° and Θ° particles.

We first examine the question of parity conservation in the Λ° decay. If parity is not conserved in the Λ° decay there is no effect in the $I(\theta)$ distribution, but there can be an up-down asymmetry in the $I(\varphi)$ distribution if the Λ° is polarized in production. At this high energy it is expected that several orbital angular momentum states will enter into the production and the polarization will in general be a

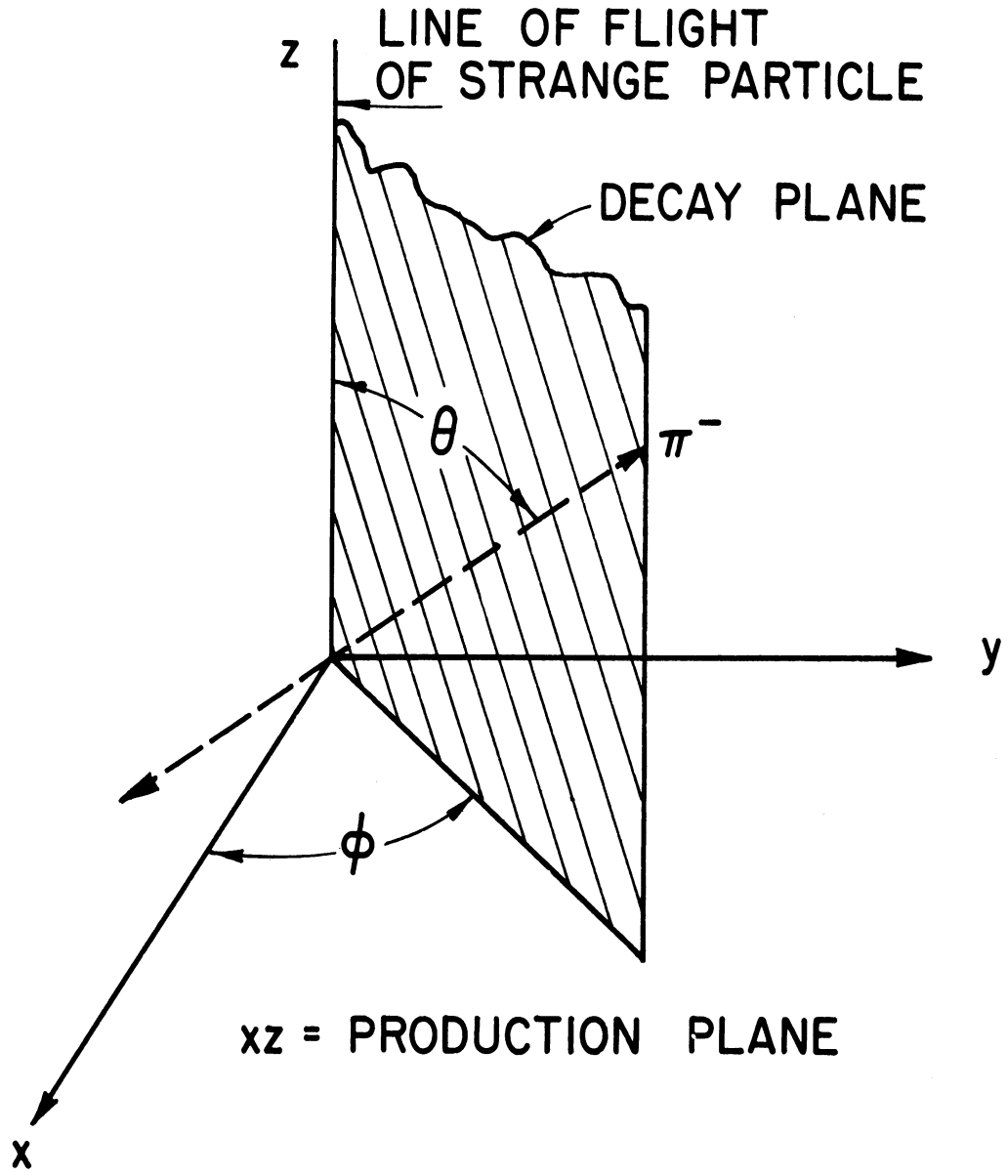

Figure 19. Coordinate System Used in Describing Strange Particle Decays.

function of the production angle. Since examining the decay distribution at all production angles can only reduce asymmetries due to parity non-conservation, any significant up-down asymmetry found in the $I(\varphi)$ distribution will definitely indicate parity violation in Λ° decay. The distribution $I(\varphi)$ for Λ° decays is presented in Figure 20. We note that there is an up-down asymmetry of 29 up and 15 down. The statistical probability that this asymmetry could have resulted from an isotropic distribution is about 5% and thus not highly significant. In order to increase the number of events and thus make a more rigorous test of parity conservation, our data have been combined with that of groups at Columbia, Bologna, and Pisa[17] who have done similar experiments but at different pion energies. From the combined data we definitely conclude that parity is not conserved in Λ° decay. This result has also been obtained by a Bevatron group of Crawford, et al.[18]. Parity non-conservation has also been detected in other weak decays such as the π and μ meson decay and in τ - θ decay (if we assume the τ and θ are the same particle). However one is puzzled by the absence of any significant indication of parity non-conservation in Σ hyperon decay[17,18], which presumably is in the same class of weak decays as the Λ° hyperon decay. A possible explanation of the experimental results is that the Σ hyperon is not polarized in production and thus parity non-conservation in its decay cannot be observed.

We next investigate the intrinsic spins of the Λ° and θ° particles by examining the experimental decay distributions $I(\theta)$ and $I(\varphi)$ for the Λ° (Figure 21) and the θ° (Figure 22). To bring out any

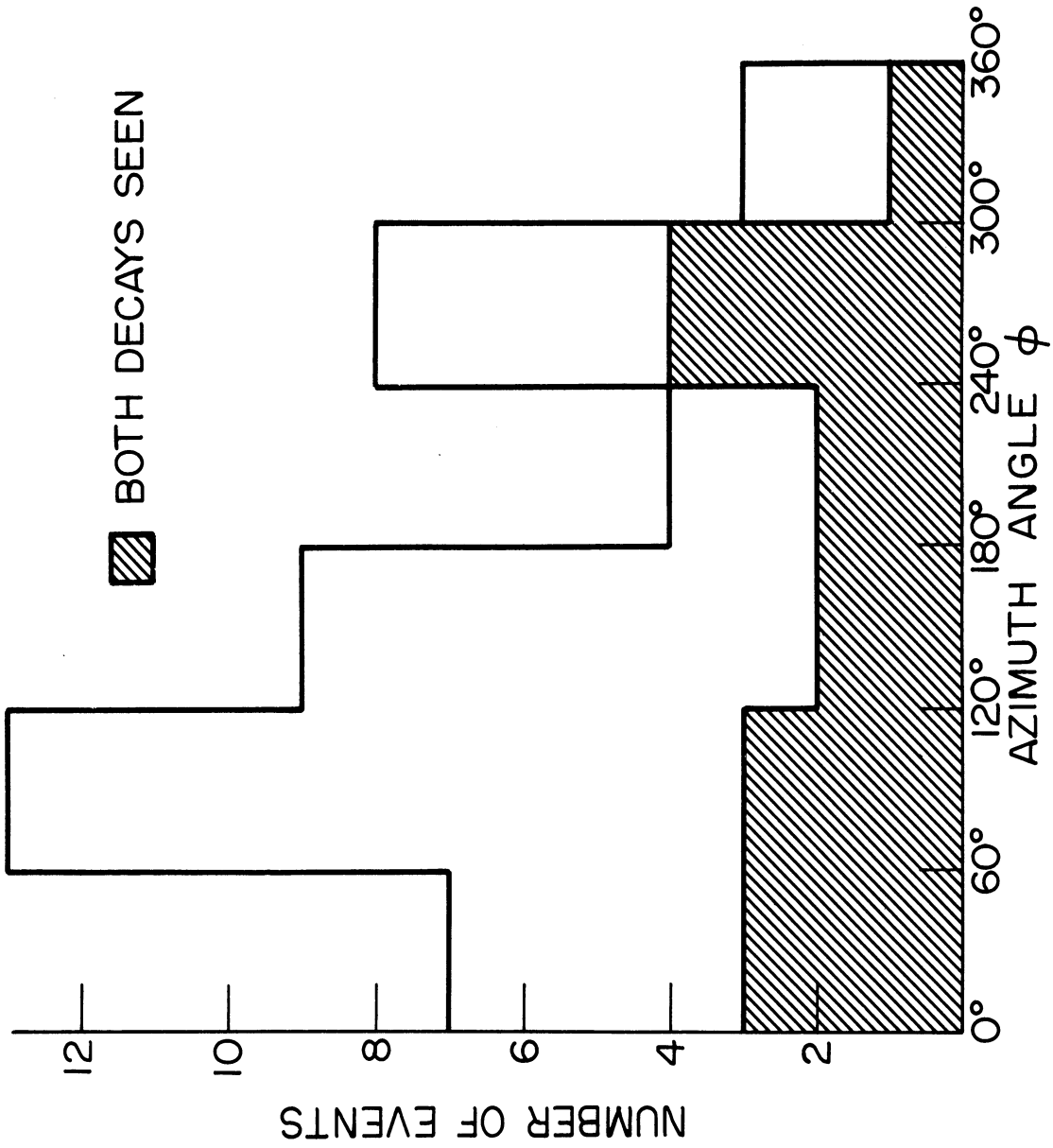

Figure 20. Distribution of Angle φ for Λ° Decay.

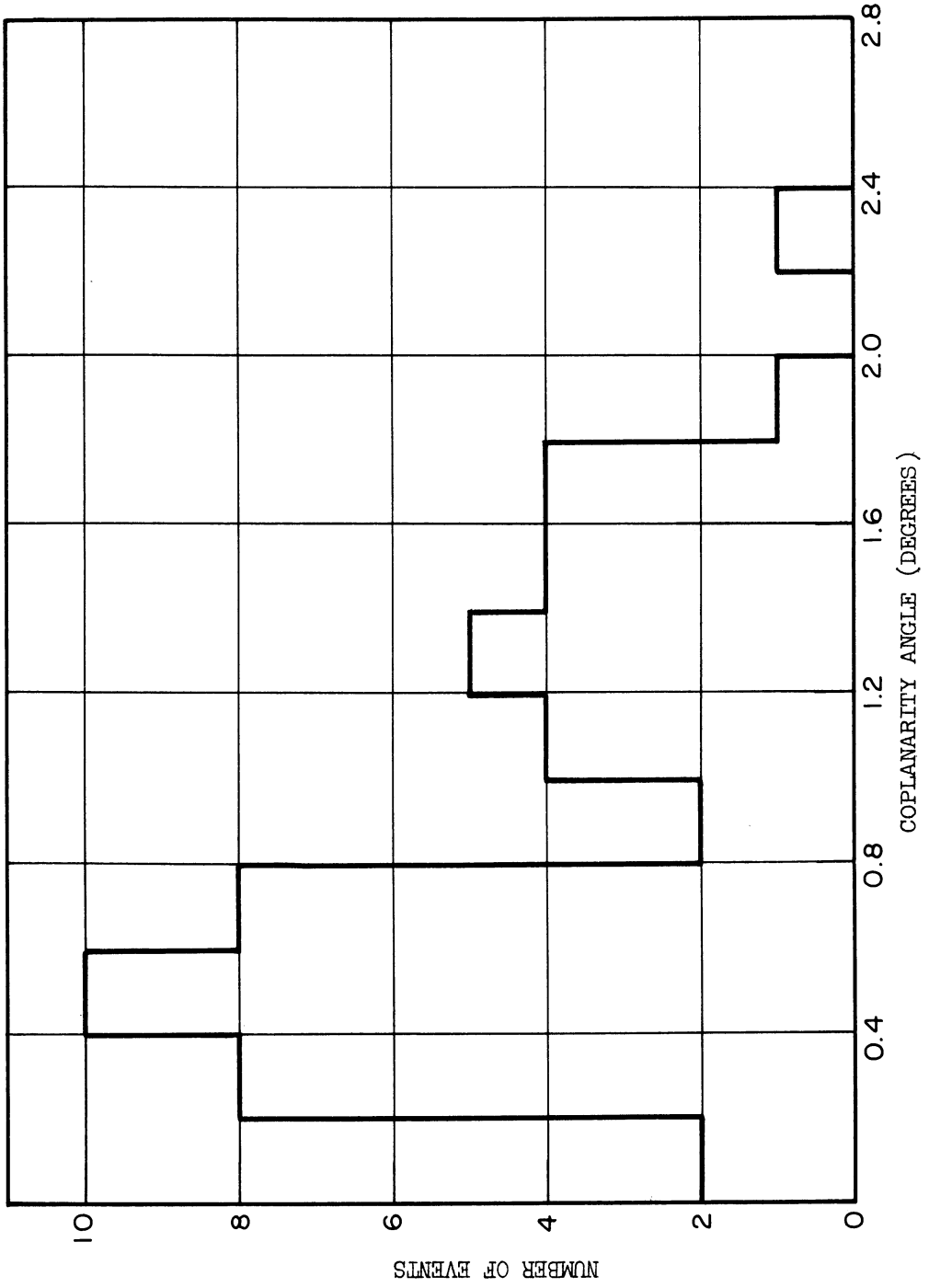

Figure 21. Folded Distribution of Angles θ and φ for Λ° Decay.

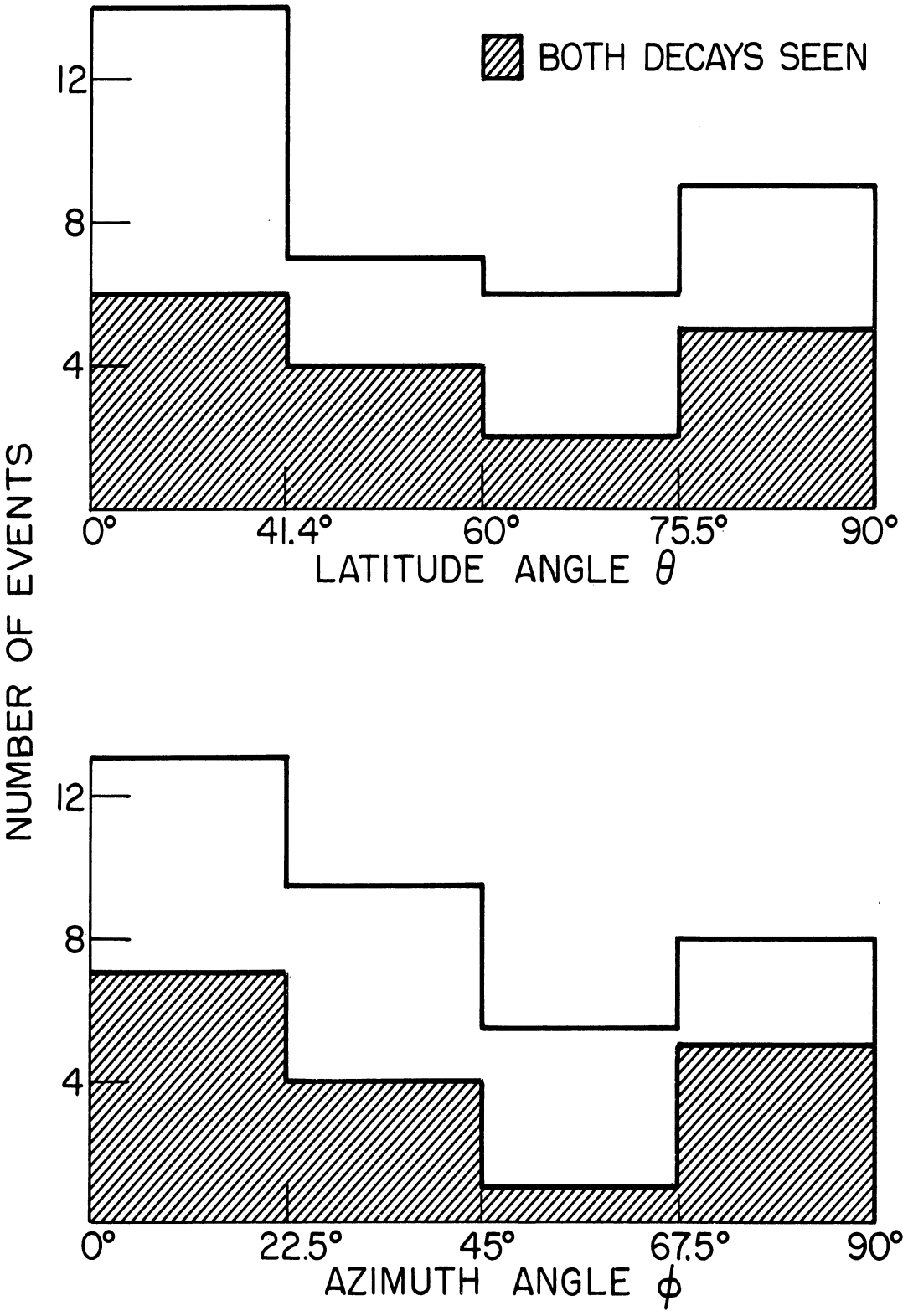

Figure 22. Folded Distribution of Angles θ and φ for θ° Decay.

anisotropy we have folded these distributions so that θ and φ run from 0 to $\pi/2$. As noted previously the polarization of the Λ° (and θ° if its spin is not zero) will in general be a function of the production angle so that considering decays at all production angles can only reduce the effect of higher order spins and thus any significant deviation of $I(\theta)$ or $I(\varphi)$ from isotropy will indicate higher order spins. Examination of Figures 21 and 22 shows no significant deviation from isotropy. For the Λ° decays from Λ° - θ° production events, the experimental $I(\theta)$ and $I(\varphi)$ distributions have respectively a 0.10 and 0.20 chi-square probability of arising from an isotropic distribution. For the θ° decays from Λ° - θ° production events the experimental $I(\theta)$ and $I(\varphi)$ distributions have respectively a 0.20 and 0.35 chi-square probability of arising from an isotropic distribution. Thus, our results are consistent with spin 1/2 for the Λ° and spin zero for the θ°. Again in order to increase the number of events our data have been combined with that of groups at Columbia, Bologna, and Pisa. The results, obtained by using the method of Adair[16], indicate that the spin of the Λ° is 1/2[19], but are not yet complete for the θ°[20].

In the analysis of Λ° parity and Λ° and θ° spins from their decay distribution we have not included those Λ°'s and θ°'s from Σ° - θ° productions since the production process may be different and the Λ° is produced by the decay of a Σ°.

5.3 Long Lived and Neutral Decay Modes

The analysis of the experimental data (the kinematical relations used) has been based upon the assumption of associated production of V°

particles, i.e., for every Λ° (or Σ°) found there is an associated θ° produced even if its decay is not seen and vice versa. This experiment does not confirm the hypothesis of associated production of strange particles but only concerns itself with those V° productions which are associated. Since our chamber is large compared to the mean decay length of the Λ° and θ° it is unlikely that all the unseen V° particles associated with those detected, decay outside the chamber by their normal charged mode. It has been theoretically postulated by Gell-Mann and Pais[21] and experimentally supported by Lande et al.[22] that half of the θ°'s produced should decay by a long lived mode. No such theoretical prediction has been made for the Λ°. Using our data we calculated the probabilities α_Λ and α_θ that the Λ° and θ decay by their normal lived charged mode.

Let $N_{\Lambda\theta}$, N_Λ, and N_θ be respectively the number of hydrogen events (i.e., after correction for carbon contamination and scanning efficiency) found where both the Λ° and θ° decayed in the chamber, where only the Λ° decayed in the chamber, and where only the θ° decayed in the chamber. Let P_Λ and P_θ be respectively the probability that a Λ° or θ°, decaying by its normal charged mode, decays before leaving the chamber. The likelihood function (L) for obtaining the events found (both single and double V°'s) can be obtained as follows. The probability of obtaining a double V° event is

$$W(\Lambda\theta) = \alpha_\Lambda\alpha_\theta P_\Lambda P_\theta ,$$

and the probability of obtaining a single V° event is

$$W(\Lambda) = \alpha_\Lambda P_\Lambda (1 - \alpha_\theta P_\theta) \quad ,$$

$$W(\theta) = \alpha_\theta P_\theta (1 - \alpha_\Lambda P_\Lambda) \quad .$$

However, since we are looking for any of these three possibilities the likelihood of obtaining a double V° event in our experiment is

$$L(\Lambda\theta) = \frac{W(\Lambda\theta)}{W(\Lambda\theta) + W(\Lambda) + W(\theta)} \quad ;$$

$$= \frac{\alpha_\Lambda \alpha_\theta P_\Lambda P_\theta}{\alpha_\Lambda P_\Lambda + \alpha_\theta P_\theta - \alpha_\Lambda \alpha_\theta P_\Lambda P_\theta} \quad ,$$

and the corresponding expressions for $\Lambda°$ and $\theta°$ events. The likelihood of obtaining $N_{\Lambda\theta}$ events, N_Λ events and N_θ events is then simply the product of these independent likelihoods. This is called the likelihood function, L.

$$L = \frac{[\alpha_\Lambda \alpha_\theta P_\Lambda P_\theta]^{N_{\Lambda\theta}} [\alpha_\Lambda P_\Lambda (1-\alpha_\theta P_\theta)]^{N_\Lambda} [\alpha_\theta P_\theta (1-\alpha_\Lambda P_\Lambda)]^{N_\theta}}{[\alpha_\Lambda P_\Lambda + \alpha_\theta P_\theta - \alpha_\Lambda \alpha_\theta P_\Lambda P_\theta]^{(N_{\Lambda\theta} + N_\Lambda + N_\theta)}}$$

The most likely values of α_Λ and α_θ are the values which maximize the likelihood function,

$$0 = \frac{\partial \ell n L}{\partial \alpha_\Lambda} = \frac{N_{\Lambda\theta} + N_\Lambda}{\alpha_\Lambda} - \frac{N_\theta P_\Lambda}{1-\alpha_\Lambda P_\Lambda} - \frac{(N_{\Lambda\theta} + N_\Lambda + N_\theta)(P_\Lambda + \alpha_\theta P_\Lambda P_\theta)}{\alpha_\Lambda P_\Lambda + \alpha_\theta P_\theta - \alpha_\Lambda \alpha_\theta P_\Lambda P_\theta}$$

$$0 = \frac{\partial \ell n L}{\partial \alpha_\theta} = \frac{N_{\Lambda\theta} + N_\theta}{\alpha_\theta} - \frac{N_\Lambda P_\theta}{1-\alpha_\theta P_\theta} - \frac{(N_{\Lambda\theta} + N_\Lambda + N_\theta)(P_\theta + \alpha_\Lambda P_\theta P_\Lambda)}{\alpha_\Lambda P_\Lambda + \alpha_\theta P_\theta - \alpha_\Lambda \alpha_\theta P_\Lambda P_\theta}$$

Solving these equations simultaneously for α_Λ and α_θ we obtain

$$\alpha_\Lambda = \frac{N_{\Lambda\theta}}{N_{\Lambda\theta} + N_\theta} \frac{1}{P_\Lambda} \quad ,$$

$$\alpha_\theta = \frac{N_{\Lambda\theta}}{N_{\Lambda\theta} + N_\Lambda} \frac{1}{P_\theta} \quad .$$

Approximately 75% of our pictures were of uniform quality and we used these to calculate α_Λ and α_θ. In this group of pictures we found the following numbers for Λ° - θ° production on hydrogen: 16 events where both the Λ° and θ° decayed in the chamber, 26 events where only the Λ° decayed in the chamber, and 17 events where only the θ° decayed inside the chamber. Correcting these numbers for scanning efficiency and carbon contamination gives $N_{\Lambda\theta} = 18.75$, $N_\Lambda = 21.32$ and $N_\theta = 30.15$. The average probability (P_Λ or P_θ) that a V° decay in the chamber was found to be 0.83. With these values we obtained

$$\alpha_\Lambda = 0.57 \pm 0.10,$$

$$\alpha_\theta = 0.46 \pm 0.10.$$

The errors are standard deviations and are primarily due to the statistical uncertainty in the number of events and uncertainties in the value of scanning efficiency and carbon contamination. These results are consistent with Plano, et.al[23], who obtained values of $\alpha_\Lambda = 0.68 \pm 0.05$ and $\alpha_\theta = 0.42 \pm 0.05$.

The value of α_θ obtained is in very good agreement with the predictions of Gell-Mann and Pias[21] that 50% of the θ°'s decay by a long lived mode (θ_2°'s) if we assume that a small fraction of the short lived θ°'s (θ_1°'s) decay by an uncharged mode. However, since the strangeness scheme of Gell-Mann[3] and Nishijima[4] is characterized by the isotopic spin selection rule $\Delta T_z = \pm 1/2$ for strange particle decay, it has been further proposed that these decays be characterized by the stronger selection rule $\Delta T = \pm 1/2$. Under this assumption one would expect that 1/3 of the θ_1°'s would decay by the uncharged mode. This is somewhat in disagreement with the experimental results. This rule also

predicts that 2/3 of the Λ°'s should decay by the charged mode. This is in much better agreement with the experimental results.

5.4 Lifetimes of the Λ° and θ° Particles

The lifetimes of the Λ° and θ° particles can be calculated using the maximum likelihood method of Bartlett[22]. Letting t_i be the time elapsed before decay for the i^{th} event (either Λ° or θ°), T_i be the potential time, i.e., the time each particle could have lived before escaping from the chamber, and τ be the unknown lifetime of the particle, the likelihood of a V° decaying at time t_i in a potential time T_i is

$$P = \frac{e^{-t_i/\tau}}{1-e^{-T_i/\tau}} \frac{1}{\tau} \quad .$$

The likelihood (L) of obtaining n V°'s decaying at times $t_1, t_2 \ldots t_n$ is then the product of these independent probabilities,

$$L(\tau) = \prod_{i=1}^{n} \frac{e^{-t_i/\tau}}{1-e^{-T_i/\tau}} \frac{1}{\tau} \quad .$$

The most likely value of the lifetime is the value of τ which maximizes the likelihood function. Λ° and θ° events are treated separately but no distinction is made between double and single V° events. Numerical tables prepared by Bartlett were used to simplify the calculation of the lifetimes. Based upon 61 cases of Λ° decay and 62 cases of θ° decay, we found

$$\tau_\theta = 0.81^{+0.23}_{-0.15} \times 10^{-10} \text{ sec.},$$

$$\tau_\Lambda = 2.08^{+0.46}_{-0.31} \times 10^{-10} \text{ sec.}$$

The errors correspond to an approximate 68% confidence limit. Potential

times were calculated up to 0.5 cm. of the chamber walls since it is probable that decays occurring closer to the walls than this would go unrecognized. No correction was made for decays occurring close to the origin (where scanning efficiency might be poor), since the distribution of "decay lengths" for V shaped objects (Figure 23) indicated no significant bias. This distribution was based upon a sample of fifty V shaped events whose "decay lengths" were under two centimeters.

5.5 Summary of Results

The properties of V° particles produced by 1.1 Bev π^- mesons on protons at rest (hydrogen events) have been studied using a 12 inch propane bubble chamber. We found the following reactions occurred

$$\pi^- + p \rightarrow \Lambda^\circ + \theta^\circ \quad ,$$

$$\pi^- + p \rightarrow \Sigma^\circ + \theta^\circ \quad ,$$

with cross sections (in milibarns) of

$$\sigma(\Lambda\theta) = 0.28 \pm 0.04 \text{ mb},$$

$$\sigma(\Sigma\theta) = 0.16 \pm 0.04 \text{ mb}.$$

In the center of mass system of production, the angular distribution of the hyperons was peaked in the backward hemisphere. The peak was more pronounced for the Λ° then for the Σ°. Combining our results with data on Σ^- and Σ^+ production at this same energy, we found that there was some indication that isotopic spin conservation may be violated in the Σ-hyperon production process.

The decay angular distributions in the center of mass system of the Λ° and θ° were examined for any indication of higher order spins and parity non-conservation. Our data were consistent with spin 1/2 for

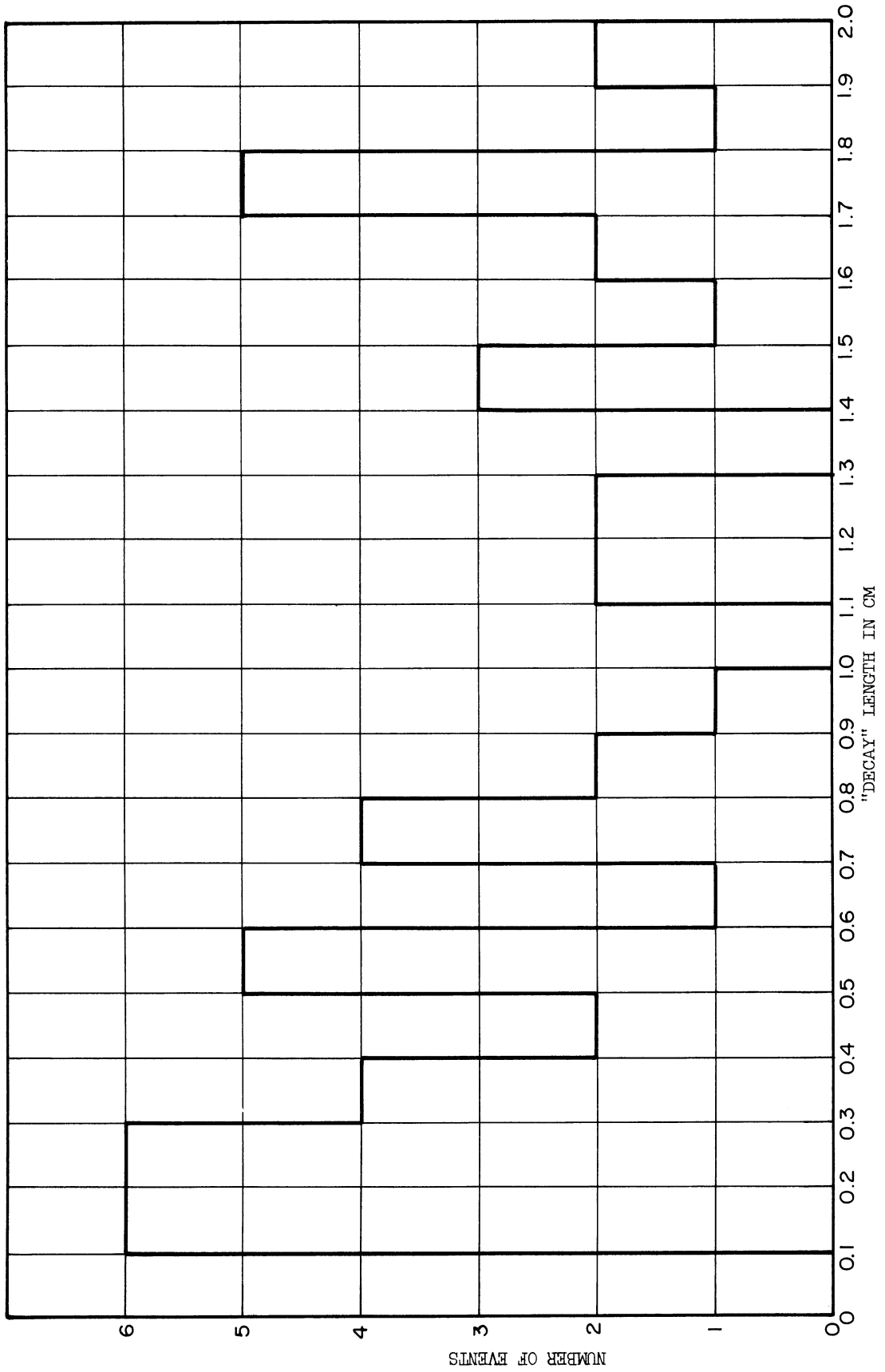

Figure 23. Distribution of "Decay" Lengths for Random Sample of V's with "Decay" Lengths Less Than 2 Centimeters.

the Λ° and spin zero for the θ°. It gave some indication of parity non-conservation in Λ° decay (about 5% significance). The limited amount of data obtained prevented more definite conclusions. However, our data combined with that of groups at Columbia, Bologna and Pisa definitely showed that the spin of the Λ° is 1/2 and that parity is not conserved in its decay. Results concerning the θ° spin are not yet complete.

From the number of events where a θ° is seen to decay without an associated Λ°, and the number of events where both the Λ° and θ° are seen to decay we concluded that the probability that the Λ° decay by its normal charged mode (α_Λ) is $\alpha_\Lambda = 0.57 \pm 0.10$. Similarly, from the number of events where a Λ° is seen to decay without an associated θ°, and the number of events where both the Λ° and θ° are seen to decay we concluded that the probability that the θ° decay by its normal charged mode (α_θ) is $\alpha_\theta = 0.46 \pm 0.10$. These results are consistent for Λ° decay with the selection rule that the total isotopic spin change by 1/2, but are somewhat inconsistent with this rule for θ° decay.

Finally we found that the lifetimes τ_Λ and τ_θ of the Λ° and θ° particles are

$$\tau_\Lambda = 2.08^{+0.46}_{-0.31} \times 10^{-10} \text{ seconds and}$$

$$\tau_\theta = 0.81^{+0.23}_{-0.15} \times 10^{-10} \text{ seconds.}$$

The errors correspond to an approximate 68% confidence limit.

These results were based upon 29 cases of the reaction $\pi^- + p \rightarrow \Lambda^\circ + \theta^\bullet$ where the Λ° was seen to decay by its normal charged mode ($\Lambda^\circ \rightarrow \pi^- + p$), 19 cases of the reaction $\pi^- + p \rightarrow \Lambda^\circ + \theta^\circ$ where the θ° was seen to decay by its normal charged mode ($\theta^\circ \rightarrow \pi^- + \pi^+$), and 11 cases of the reaction $\pi^- + p \rightarrow \Sigma^\circ + \theta^\circ$ where the θ° was seen to decay by its normal charged mode. In addition we included for completeness in our analysis 17 cases of the reaction $\pi^- + p \rightarrow \Lambda^\circ + \theta^\circ$ and 15 cases of the reaction $\pi^- + p \rightarrow \Sigma^\circ + \theta^\circ$ where both the Λ° and θ° decayed in the chamber. These later cases were previously reported on and are not part of our work.

APPENDIX

LIST OF DATA

The production and decay angles for all single V° events is given below. The angles are defined in Section 5.1 and Section 5.2.

Single Λ° Events From Λ° - Θ° Productions

Event	Pro. Angle (deg.)	Decay Angle θ (deg.)	Decay Angle φ (deg.)
14236	139	62	317
15291	155	152	7
15416	100	90	88
15611	92	135	275
15767	113	123	33
17979	125	124	70
19860	90	82	112
20319	133	72	35
22544	75	48	142
24121	115	38	143
24570	108	72	243
26803	157	116	118
26885	143	123	97
28231	30	52	67
28304	58	49	155
30172	111	114	195
31316	3	68	226
31335	90	61	141
32084	149	119	75
33081	39	163	121
34217	58	90	100
34239	91	100	80
35972	174	79	266
36274	152	52	140
37708	111	99	317
39087	145	56	63
12911	163	148	124
16436	38	69	263
19808	125	142	34

Single θ° Events From Λ° - θ° Productions

Event	Pro. Angle (deg.)	Decay Angle θ (deg.)	Decay Angle φ (deg.)
14664	174	78	135
19028	156	79	115
20044	134	88	184
21131	42	62	54
22278	82	18	136
23078	88	36	312
24712	131	74	181
25754	145	25	290
26999	139	15	153
27368	146	5	154
28476	157	35	227
33002	118	28	313
34866	78	25	167
36393	161	47	36
37613	125	49	339
37739	100	85	17
39078	88	52	83
13159	113	65	203
16102	147	67	175

Single θ° Events From Σ° - θ° Productions

Event	Pro. Angle (deg.)	Decay Angle θ (deg.)	Decay Angle φ (deg.)
19264	132	33	80
19707	122	42	175
19816	122	70	3
22335	140	60	78
28519	100	14	171
29613	60	29	40
29955	152	19	77
30496	110	77	32
31634	78	88	10
33098	52	17	134
38544	60	51	93

BIBLIOGRAPHY

1. Rochester and Butler, Nature, 160, 855 (1947).

2. Pais, Phys. Rev. 86, 663 (1952).

3. Gell-Mann, M., Phys. Rev. 92, 833 (1953).

4. Nishijima, Progr. Theor. Phys. 9, 414 (1953).

5. Fowler, Shutt, Thorndike, and Whittemore, Phys. Rev. 91, 1287 (1953).

6. Walker, Phys. Rev. 98, 1407 (1955) and Walker and Shephard, Phys. Rev. 101, 1810 (1956).

7. R. Budde, M. Chretien, J. Leitner, H. Samios, M. Schwartz, and J. Steinberger, Phys. Rev. 103, 1827 (1956).

8. J. Brown, D. Glaser, M. Perl, Phys. Rev. 108, 1036 (1957).

9. D. C. Rahm, thesis, The University of Michigan, 1956(unpublished).

10. Glaser, Rahm, and Dodd, Phys. Rev. 102, 1653 (1956).

11. Cronin, Glaser, and Vander Velde, International Conference on Mesons and Recently Discovered Particles, Venice, Spetember 1957.

12. Cronin, Cool and Abashian, Phys. Rev., 107, 1121 (1957); Cool, Piccioni, and Clark, Phys. Rev. 103, 1082 (1956).

13. Brown, Glaser, Meyer, Perl, Vander Velde and Cronin, Phys. Rev. 107, 906 (1957).

14. Lee, Steinberger, Feinberg, Kabir, and Yang, Phys. Rev. 106, 1367 (1957).

15. Morpugo, Nuovo Cimento, 4, 1222 (1956), and 3, 1069 (1956).

16. Adair, Phys. Rev. 100, 1540 (1955).

17. F. Eisler, R. Plano, A. Prodell, N. Samios, M. Schwartz, J. Steinberger, P. Bassi, V. Borelli, G. Puppi, G. Tanaka, P. Woloschek, V. Zoboli, M. Conversi, P. Franzini, I. Mannelli, R. Santangelo, V. Silvestrini, D. A. Glaser, C. Graves, and M. L. Perl, Phys. Rev. 108, 1353 (1957).

18. F. Crawford, Jr., M. Cresti, M. Good, K. Gottstein, E. Lyman, F. Solmitz, M. Stevenson, and H. Ticho, Phys. Rev. 108, 1102 (1957).

19. F. Eisler, R. Plano, A. Prodell, N. Samios, M. Schwartz, J. Steinberger, P. Bassi, V. Borelli, G. Puppi, G. Tanaka, P. Woloschek, V. Zoboli, M. Conversi, P. Franzini, I. Mannelli, R. Santangelo, V. Silvestrini, J. L. Brown, D. A. Glaser, C. Graves, International Conference on Mesons and Recently Discovered Particles, Venice, September 1957.

20. F. Eisler, R. Plano, A. Prodell, N. Samios, M. Schwartz, J. Steinberger, P. Bassi, V. Borelli, G. Puppi, G. Tanaka, P. Woloschek, V. Zoboli, M. Conversi, P. Franzini, I. Mannelli, R. Santangelo, V. Silvestrini, J. L. Brown, D. A. Glaser, C. Graves, International Conference on Mesons and Recently Discovered Particles, Venice, September 1957.

21. M. Gell-Mann and A. Pais, Phys. Rev. 97, 1387 (1955).

22. Lande, Booth, Impeduglia, Lederman, and Chinowsky, Phys. Rev. 103, 1901 (1956).

23. R. Plano, N. Samios, M. Schwartz, J. Steinberger, and F. Eisler, Nevis Report R173.

24. M. S. Bartlett, Phil. Mag. 44, 249 (1953).